Correction notice

Universal computing by DNA origami robots in a living animal

Yaniv Amir, Eldad Ben-Ishay, Daniel Levner, Shmulik Ittah, Almogit Abu-Horowitz and Ido Bachelet

Nature Nanotechnology http://dx.doi.org/10.1038/nnano.2014.58 (2014)

In the version of the Supplementary Information originally published online, Supplementary Note 6 was missing. This error has been corrected in this file 17 April 2014.

DOI: 10.1038/NNANO.2014.58

Universal computing by DNA origami robots in a living animal

Supplementary Note 5: Statistical mechanics of robots in the hemocoel

Supplementary Note 6: Scaling of complexity and error

Supplementary Table 1: Truth tables and effector complexes

Architecture	X	Y	Output	Effector complexes
E (AND)	0	0	0	
	1	0	0	
	0	1	0	
	1	1	1	E
EP1P2 (OR)	0	0	0	
	1	0	1	EP1
	0	1	1	EP2
	1	1	1	E, EP1, EP2, EP1P2
EP1P2N (XOR)	0	0	0	
	1	0	1	EP1
	0	1	1	EP2
	1	1	0	EN
E_{open}N (NAND)	0	0	1	E
	1	0	1	E
	0	1	1	E
	1	1	0	EN
$E_{open}N_X$ (NOT)	0		1	E
	1		0	EN

	X	Y	Output 1	Output 2	Effector complexes
EFP1P2P3N (CNOT)	0	0	0	0	
	1	0	1	0	EP1
	0	1	1	1	EP2+F
	1	1	0	1	EN+F

Supplementary Note 1: Robot design and folding:

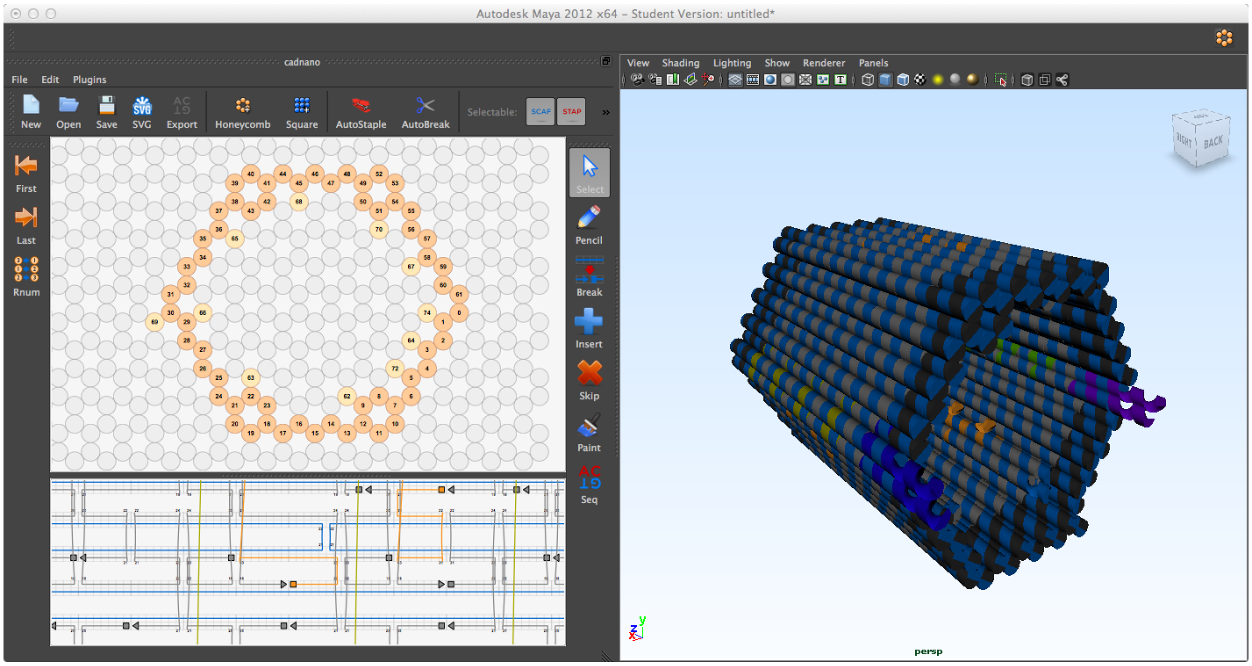

Supplementary Fig. 1: Design interface screenshot (produced by caDNAno[15] (http://cadnano.org/)). The robot caDNAno file (.json format) is available to download as a supplementary file.

Supplementary Fig. 2: Sequence of M13mp18 DNA scaffold:

M13mp18 DNA[16] was purchased from New England Biolabs (NEB #N4040), scaffold is a 7249bp circular single-strand DNA molecule

```
>M13mp18_p7249
AATGCTACTACTATTAGTAGAATTGATGCCACCTTTTCAGCTCGCGCCCCAAATGAAAATATAGCTAAACAGGTTATTG
ACCATTTGCGAAATGTATCTAATGGTCAAACTAAATCTACTCGTTCGCAGAATTGGGAATCAACTGTTATATGGAATGA
AACTTCCAGACACCGTACTTTAGTTGCATATTTAAAACATGTTGAGCTACAGCATTATATTCAGCAATTAAGCTCTAAG
CCATCCGCAAAAATGACCTCTTATCAAAAGGAGCAATTAAAGGTACTCTCTAATCCTGACCTGTTGGAGTTTGCTTCCG
GTCTGGTTCGCTTTGAAGCTCGAATTAAAACGCGATATTTGAAGTCTTTCGGGCTTCCTCTTAATCTTTTTGATGCAATC
CGCTTTGCTTCTGACTATAATAGTCAGGGTAAAGACCTGATTTTTGATTTATGGTCATTCTCGTTTTCTGAACTGTTTAAA
GCATTTGAGGGGGATTCAATGAATATTTATGACGATTCCGCAGTATTGGACGCTATCCAGTCTAAACATTTTACTATTAC
CCCCTCTGGCAAAACTTCTTTTGCAAAAGCCTCTCGCTATTTTGGTTTTTATCGTCGTCTGGTAAACGAGGGTTATGATA
GTGTTGCTCTTACTATGCCTCGTAATTCCTTTTGGCGTTATGTATCTGCATTAGTTGAATGTGGTATTCCTAAATCTCAAC
TGATGAATCTTTCTACCTGTAATAATGTTGTTCCGTTAGTTCGTTTTATTAACGTAGATTTTTCTTCCCAACGTCCTGACT
GGTATAATGAGCCAGTTCTTAAAATCGCATAAGGTAATTCACAATGATTAAAGTTGAAATTAAACCATCTCAAGCCCAA
TTTACTACTCGTTCTGGTGTTTCTCGTCAGGGCAAGCCTTATTCACTGAATGAGCAGCTTTGTTACGTTGATTTGGGTAA
TGAATATCCGGTTCTTGTCAAGATTACTCTTGATGAAGGTCAGCCAGCCTATGCGCCTGGTCTGTACACCGTTCATCTGT
CCTCTTTCAAAGTTGGTCAGTTCGGTTCCCTTATGATTGACCGTCTGCGCCTCGTTCCGGCTAAGTAACATGGAGCAGGT
CGCGGATTTCGACACAATTTATCAGGCGATGATACAAATCTCCGTTGTACTTTGTTTCGCGCTTGGTATAATCGCTGGGG
GTCAAAGATGAGTGTTTTAGTGTATTCTTTTGCCTCTTTCGTTTTAGGTTGGTGCCTTCGTAGTGGCATTACGTATTTTAC
CCGTTTAATGGAAACTTCCTCATGAAAAAGTCTTTAGTCCTCAAAGCCTCTGTAGCCGTTGCTACCCTCGTTCCGATGCT
GTCTTTCGCTGCTGAGGGTGACGATCCCGCAAAAGCGGCCTTTAACTCCCTGCAAGCCTCAGCGACCGAATATATCGGT
TATGCGTGGGCGATGGTTGTTGTCATTGTCGGCGCAACTATCGGTATCAAGCTGTTTAAGAAATTCACCTCGAAAGCAA
GCTGATAAACCGATACAATTAAAGGCTCCTTTTGGAGCCTTTTTTTTGGAGATTTTCAACGTGAAAAAATTATTATTCGC
AATTCCTTTAGTTGTTCCTTTCTATTCTCACTCCGCTGAAACTGTTGAAAGTTGTTTAGCAAAATCCCATACAGAAAATT
CATTTACTAACGTCTGGAAAGACGACAAAACTTTAGATCGTTACGCTAACTATGAGGGCTGTCTGTGGAATGCTACAGG
CGTTGTAGTTTGTACTGGTGACGAAACTCAGTGTTACGGTACATGGGTTCCTATTGGGCTTGCTATCCCTGAAAATGAG
GGTGGTGGCTCTGAGGGTGGCGGTTCTGAGGGTGGCGGTTCTGAGGGTGGCGGTACTAAACCTCCTGAGTACGGTGAT
ACACCTATTCCGGGCTATACTTATATCAACCCTCTCGACGGCACTTATCCGCCTGGTACTGAGCAAAACCCCGCTAATC
CTAATCCTTCTCTTGAGGAGTCTCAGCCTCTTAATACTTTCATGTTTCAGAATAATAGGTTCCGAAATAGGCAGGGGGC
ATTAACTGTTTATACGGGCACTGTTACTCAAGGCACTGACCCCGTTAAAACTTATTACCAGTACACTCCTGTATCATCAA
AAGCCATGTATGACGCTTACTGGAACGGTAAATTCAGAGACTGCGCTTTCCATTCTGGCTTTAATGAGGATTTATTTGTT
TGTGAATATCAAGGCCAATCGTCTGACCTGCCTCAACCTCCTGTCAATGCTGGCGGCGGCTCTGGTGGTGGTTCTGGTG
GCGGCTCTGAGGGTGGTGGCTCTGAGGGTGGCGGTTCTGAGGGTGGCGGCTCTGAGGGAGGCGGTTCCGGTGGTGGCT
CTGGTTCCGGTGATTTTGATTATGAAAAGATGGCAAACGCTAATAAGGGGGCTATGACCGAAAATGCCGATGAAAACG
CGCTACAGTCTGACGCTAAAGGCAAACTTGATTCTGTCGCTACTGATTACGGTGCTGCTATCGATGGTTTCATTGGTGAC
GTTTCCGGCCTTGCTAATGGTAATGGTGCTACTGGTGATTTTGCTGGCTCTAATTCCCAAATGGCTCAAGTCGGTGACGG
TGATAATTCACCTTTAATGAATAATTTCCGTCAATATTTACCTTCCCTCCCTCAATCGGTTGAATGTCGCCCTTTTGTCTT
TGGCGCTGGTAAACCATATGAATTTTCTATTGATTGTGACAAAATAAACTTATTCCGTGGTGTCTTTGCGTTTCTTTTAT
ATGTTGCCACCTTTATGTATGTATTTTCTACGTTTGCTAACATACTGCGTAATAAGGAGTCTTAATCATGCCAGTTCTTTT
GGGTATTCCGTTATTATTGCGTTTCCTCGGTTTCCTTCTGGTAACTTTGTTCGGCTATCTGCTTACTTTTCTTAAAAAGGG
CTTCGGTAAGATAGCTATTGCTATTTCATTGTTTCTTGCTCTTATTATTGGGCTTAACTCAATTCTTGTGGGTTATCTCTC
TGATATTAGCGCTCAATTACCCTCTGACTTTGTTCAGGGTGTTCAGTTAATTCTCCCGTCTAATGCGCTTCCCTGTTTTTA
TGTTATTCTCTCTGTAAAGGCTGCTATTTTCATTTTTGACGTTAAACAAAAAATCGTTTCTTATTTGGATTGGGATAAAT
AATATGGCTGTTTATTTTGTAACTGGCAAATTAGGCTCTGGAAAGACGCTCGTTAGCGTTGGTAAGATTCAGGATAAAA
TTGTAGCTGGGTGCAAAATAGCAACTAATCTTGATTTAAGGCTTCAAAACCTCCCGCAAGTCGGGAGGTTCGCTAAAAC
GCCTCGCGTTCTTAGAATACCGGATAAGCCTTCTATATCTGATTTGCTTGCTATTGGGCGCGGTAATGATTCCTACGATG
AAAATAAAAACGGCTTGCTTGTTCTCGATGAGTGCGGTACTTGGTTTAATACCCGTTCTTGGAATGATAAGGAAAGACA
GCCGATTATTGATTGGTTTCTACATGCTCGTAAATTAGGATGGGATATTATTTTTCTTGTTCAGGACTTATCTATTGTTGA
TAAACAGGCGCGTTCTGCATTAGCTGAACATGTTGTTTATTGTCGTCGTCTGGACAGAATTACTTTACCTTTTGTCGGTA
CTTTATATTCTCTTATTACTGGCTCGAAAATGCCTCTGCCTAAATTACATGTTGGCGTTGTTAAATATGGCGATTCTCAA
TTAAGCCCTACTGTTGAGCGTTGGCTTTATACTGGTAAGAATTTGTATAACGCATATGATACTAAACAGGCTTTTTCTAG
TAATTATGATTCCGGTGTTTATTCTTATTTAACGCCTTATTTATCACACGGTCGGTATTTCAAACCATTAAATTTAGGTCA
GAAGATGAAATTAACTAAAATATATTTGAAAAAGTTTTCTCGCGTTCTTTGTCTTGCGATTGGATTTGCATCAGCATTTA
CATATAGTTATATAACCCAACCTAAGCCGGAGGTTAAAAAGGTAGTCTCTCAGACCTATGATTTTGATAAATTCACTAT
TGACTCTTCTCAGCGTCTTAATCTAAGCTATCGCTATGTTTTCAAGGATTCTAAGGGAAAATTAATTAATAGCGACGATT
TACAGAAGCAAGGTTATTCACTCACATATATTGATTTATGTACTGTTTCCATTAAAAAAGGTAATTCAAATGAAATTGTT
AAATGTAATTAATTTTGTTTTCTTGATGTTTGTTTCATCATCTTCTTTTGCTCAGGTAATTGAAATGAATAATTCGCCTCT
GCGCGATTTTGTAACTTGGTATTCAAAGCAATCAGGCGAATCCGTTATTGTTTCTCCCGATGTAAAAGGTACTGTTACTG
TATATTCATCTGACGTTAAACCTGAAAATCTACGCAATTTCTTTATTTCTGTTTTACGTGCAAATAATTTTGATATGGTA
GGTTCTAACCCTTCCATTATTCAGAAGTATAATCCAAACAATCAGGATTATATTGATGAATTGCCATCATCTGATAATCA
GGAATATGATGATAATTCCGCTCCTTCTGGTGGTTTCTTTGTTCCGCAAAATGATAATGTTACTCAAACTTTTAAAATTA
ATAACGTTCGGGCAAAGGATTTAATACGAGTTGTCGAATTGTTTGTAAAGTCTAATACTTCTAAATCCTCAAATGTATT
ATCTATTGACGGCTCTAATCTATTAGTTGTTAGTGCTCCTAAAGATATTTTAGATAACCTTCCTCAATTCCTTTCAACTGT
TGATTTGCCAACTGACCAGATATTGATTGAGGGTTTGATATTTGAGGTTCAGCAAGGTGATGCTTTAGATTTTTCATTTG
```

CTGCTGGCTCTCAGCGTGGCACTGTTGCAGGCGGTGTTAATACTGACCGCCTCACCTCTGTTTTATCTTCTGCTGGTGGT
TCGTTCGGTATTTTTAATGGCGATGTTTTAGGGCTATCAGTTCGCGCATTAAAGACTAATAGCCATTCAAAAATATTGTC
TGTGCCACGTATTCTTACGCTTTCAGGTCAGAAGGGTTCTATCTCTGTTGGCCAGAATGTCCCTTTTATTACTGGTCGTG
TGACTGGTGAATCTGCCAATGTAAATAATCCATTTCAGACGATTGAGCGTCAAAATGTAGGTATTTCCATGAGCGTTTT
TCCTGTTGCAATGGCTGGCGGTAATATTGTTCTGGATATTACCAGCAAGGCCGATAGTTTGAGTTCTTCTACTCAGGCAA
GTGATGTTATTACTAATCAAAGAAGTATTGCTACAACGGTTAATTTGCGTGATGGACAGACTCTTTTACTCGGTGGCCTC
ACTGATTATAAAAACACTTCTCAGGATTCTGGCGTACCGTTCCTGTCTAAAATCCCTTTAATCGGCCTCCTGTTTAGCTC
CCGCTCTGATTCTAACGAGGAAAGCACGTTATACGTGCTCGTCAAAGCAACCATAGTACGCGCCCTGTAGCGGCGCATT
AAGCGCGGCGGGTGTGGTGGTTACGCGCAGCGTGACCGCTACACTTGCCAGCGCCCTAGCGCCCGCTCCTTTCGCTTTC
TTCCCTTCCTTTCTCGCCACGTTCGCCGGCTTTCCCCGTCAAGCTCTAAATCGGGGGCTCCCTTTAGGGTTCCGATTTAGT
GCTTTACGGCACCTCGACCCCAAAAAACTTGATTTGGGTGATGGTTCACGTAGTGGGCCATCGCCCTGATAGACGGTTT
TTCGCCCTTTGACGTTGGAGTCCACGTTCTTTAATAGTGGACTCTTGTTCCAAACTGGAACAACACTCAACCCTATCTCG
GGCTATTCTTTTGATTTATAAGGGATTTTGCCGATTTCGGAACCACCATCAAACAGGATTTTCGCCTGCTGGGGCAAACC
AGCGTGGACCGCTTGCTGCAACTCTCTCAGGGCCAGGCGGTGAAGGGCAATCAGCTGTTGCCCGTCTCACTGGTGAAA
AGAAAAACCACCCTGGCGCCCAATACGCAAACCGCCTCTCCCCGCGCGTTGGCCGATTCATTAATGCAGCTGGCACGA
CAGGTTTCCCGACTGGAAAGCGGGCAGTGAGCGCAACGCAATTAATGTGAGTTAGCTCACTCATTAGGCACCCCAGGC
TTTACACTTTATGCTTCCGGCTCGTATGTTGTGTGGAATTGTGAGCGGATAACAATTTCACACAGGAAACAGCTATGAC
CATGATTACGAATTCGAGCTCGGTACCCGGGGATCCTCTAGAGTCGACCTGCAGGCATGCAAGCTTGGCACTGGCCGTC
GTTTTACAACGTCGTGACTGGGAAAACCCTGGCGTTACCCAACTTAATCGCCTTGCAGCACATCCCCCTTTCGCCAGCT
GGCGTAATAGCGAAGAGGCCCGCACCGATCGCCCTTCCCAACAGTTGCGCAGCCTGAATGGCGAATGGCGCTTTGCCT
GGTTTCCGGCACCAGAAGCGGTGCCGGAAAGCTGGCTGGAGTGCGATCTTCCTGAGGCCGATACTGTCGTCGTCCCCTC
AAACTGGCAGATGCACGGTTACGATGCGCCCATCTACACCAACGTGACCTATCCCATTACGGTCAATCCGCCGTTTGTT
CCCACGGAGAATCCGACGGGTTGTTACTCGCTCACATTTAATGTTGATGAAAGCTGGCTACAGGAAGGCCAGACGCGA
ATTATTTTTGATGGCGTTCCTATTGGTTAAAAAATGAGCTGATTTAACAAAAATTTAATGCGAATTTTAACAAAATATTA
ACGTTTACAATTTAAATATTTGCTTATACAATCTTCCTGTTTTTGGGGCTTTTCTGATTATCAACCGGGGTACATATGATT
GACATGCTAGTTTTACGATTACCGTTCATCGATTCTCTTGTTTGCTCCAGACTCTCAGGCAATGACCTGATAGCCTTTGT
AGATCTCTCAAAAATAGCTACCCTCTCCGGCATTAATTTATCAGCTAGAACGGTTGAATATCATATTGATGGTGATTTG
ACTGTCTCCGGCCTTTCTCACCCTTTTGAATCTTTACCTACACATTACTCAGGCATTGCATTTAAAATATATGAGGGTTCT
AAAAATTTTTATCCTTGCGTTGAAATAAAGGCTTCTCCCGCAAAAGTATTACAGGGTCATAATGTTTTTGGTACAACCG
ATTTAGCTTTATGCTCTGAGGCTTTATTGCTTAATTTTGCTAATTCTTTGCCTTGCCTGTATGATTTATTGGATGTT

Supplementary Fig. 3: Robot staple sequences

Staples were purchased from Integrated DNA Technologies, reconstituted in ultrapure, DNase/RNase-free water to 100 µM concentration and stored at -20 °C. All sequences are in the 5' to 3' direction.

ID	Description		Sequence
1	core		AAAAACCAAACCCTCGTTGTGAATATGGTTTGGTC
2	core		GGAAGAAGTGTAGCGGTCACGTTATAATCAGCAGACTGATAG
3	core		TACGATATAGATAATCGAACAACA
4	core		CTTTTGCTTAAGCAATAAAGCGAGTAGA
5	core		GTCTGAAATAACATCGGTACGGCCGCGCACGG
6	core		GGAAGAGCCAAACAGCTTGCAGGGAACCTAA
7	core		AAAATCACCGGAAGCAAACTCTGTAGCT
8	core		CCTACATGAAGAACTAAAGGGCAGGGCGGAGCCCCGGGC
9	core		CATGTAAAAAGGTAAAGTAATAAGAACG
10	core		ATTAAATCAGGTCATTGCCTGTCTAGCTGATAAATTGTAATA
11	core		ATAGTCGTCTTTTGCGGTAATGCC
12	core		AGTCATGGTCATAGCTGAACTCACTGCCAGT
13	core		AACTATTGACGGAAATTTGAGGGAATATAAA
14	core		ATCGCGTCTGGAAGTTTCATTCCATATAGAAAGACCATC
15	core		AAATATTGAACGGTAATCGTAGCCGGAGACAGTCATAAAAAT
16	core		GTCTTTACAGGATTAGTATTCTAACGAGCATAGAACGC
17	core		GCACCGCGACGACGCTAATGAACAGCTG
18	core		AACTTCATTTTAGAATCGCAAATC
19	core		CGTAGAGTCTTTGTTAAGGCCTTCGTTTTCCTACCGAG
20	core		CCAATCAAAGGCTTATCCGGTTGCTATT
21	core		AGAGGCGATATAATCCTGATTCATCATA
22	core		CCGTAATCCCTGAATAATAACGGAATACTACG
23	core		AAATGGTATACAGGGCAAGGAAATC
24	core		TCCTCATCGTAACCAAGACCGACA
25	core		CATTATCTGGCTTTAGGGAATTATGTTTGGATTAC
26	core		ACCCGCCCAATCATTCCTCTGTCC
27	core		CGACCAGTCACGCAGCCACCGCTGGCAAAGCGAAAGAAC
28	core		CTAAAGGCGTACTATGGTTGCAACAGGAGAGA
29	core		TTGGCAGGCAATACAGTGTTTCTGCGCGGGCG
30	core		TATACAGGAAATAAAGAAATTTTGCCCGAACGTTAAGACTTT
31	core		AAGTATAGTATAAACAGTTAACTGAATTTACCGTTGAGCCAC
32	core		ACATTCAGATAGCGTCCAATATTCAGAA
33	core		AAACATCTTTACCCTCACCAGTAAAGTGCCCGCCC
34	core		GAGATGACCCTAATGCCAGGCTATTTTT
35	core		TCCTGAATTTTTTGTTTAACGATCAGAGCGGA
36	core		GCCGAAAAATCTAAAGCCAATCAAGGAAATA
37	core		AGCGTAGCGCGTTTTCACAAAATCTATGTTAGCAAACGAACGCAAC AAA
38	core		ACCAATCGATTAAATTGCGCCATTATTA
39	core		ATCTTACTTATTTTCAGCGCCGACAGGATTCA
40	core		CCCTAAAAGAACCCAGTCACA

41	core		GGAAGGGCGAAAATCGGGTTTTTCGCGTTGCTCGT
42	core		CAGACCGGAAGCCGCCATTTTGATGGGGTCAGTAC
43	core		TAATATTGGAGCAAACAAGAGATCAATATGATATTGCCTTTA
44	core		TTCCTTATAGCAAGCAAATCAAATTTTA
45	core		ACTACGAGGAGATTTTTTCACGTTGAAACTTGCTTT
46	core		AAACAGGCATGTCAATCATATAGATTCAAAAGGGTTATATTT
47	core		AACAGGCACCAGTTAAAGGCCGCTTTGTGAATTTCTTA
48	core		TTCCTGAGTTATCTAAAATATTCAGTTGTTCAAATAGCAG
49	core		AAAGAAACAAGAGAAGATCCGGCT
50	core		TTGAGGGTTCTGGTCAGGCTGTATAAGC
51	core		TTTAACCGTCAATAGTGAATTCAAAAGAAGATGATATCGCGC
52	core		ACGAGCGCCCAATCCAAATAAAATTGAGCACC
53	core		AATAAGTCGAAGCCCAATAATTATTTATTCTT
54	core		ACGAAATATCATAGATTAAGAAACAATGGAACTGA
55	core		TTTCATAGTTGTACCGTAACACTGGGGTTTT
56	core		AGGAGCGAGCACTAACAACTAAAACCCTATCACCTAACAGTG
57	core		CAAAGTATTAATTAGCGAGTTTCGCCACAGAACGA
58	core		TGGGGAGCTATTTGACGACTAAATACCATCAGTTT
59	core		ATAACGCAATAGTAAAATGTTTAAATCA
60	core		ACGAATCAACCTTCATCTTATACCGAGG
61	core		TAATGGTTTGAAATACGCCAA
62	core		CGGAACAAGAGCCGTCAATAGGCACAGACAATATCCTCAATC
63	core		ATTAAAGGTGAATTATCAAAGGGCACCACGG
64	core		GGCAACCCATAGCGTAAGCAGCGACCATTAA
65	core		AGAAACGTAAGCAGCCACAAGGAAACGATCTT
66	core		AGAGGTCTTTAGGGGGTCAAAAGGCAGT
67	core		GGGGACTTTTTCATGAGGACCTGCGAGAATAGAAAGGAGGAT
68	core		TTTTAGAACATCCAATAAATCCAATAAC
69	core		AAATGTGGTAGATGGCCCGCTTGGGCGC
70	core		ACGGATCGTCACCCTCACGATCTAGAATTTT
71	core		CGCCATAAGACGACGACAATAGCTGTCT
72	core		GCGTATTAGTCTTTAATCGTAAGAATTTACA
73	core		AGAGAACGTGAATCAAATGCGTATTTCCAGTCCCC
74	core		AACGAAAAAGCGCGAAAAAAAGGCTCCAAAAGG
75	core		TAATTTAGAACGCGAGGCGTTAAGCCTT
76	core		ACCAGGCGTGCATCATTAATTTTTTCAC
77	core		CAGCCTGACGACAGATGTCGCCTGAAAT
78	core		ATTAGTCAGATTGCAAAGTAAGAGTTAAGAAGAGT
79	core		CTCGAATGCTCACTGGCGCAT
80	core		GGGCAGTCACGACGTTGAATAATTAACAACC
81	core		TAAAAACAGGGGTTTTGTTAGCGAATAATATAATAGAT
82	core		TCAACCCTCAGCGCCGAATATATTAAGAATA
83	core		ATTATACGTGATAATACACATTATCATATCAGAGA
84	core		GCAAATCTGCAACAGGAAAAATTGC
85	core		ATAATTACTAGAAATTCTTAC
86	core		TATCACCGTGCCTTGAGTAACGCGTCATACATGGCCCCTCAG
87	core		AAGTAGGGTTAACGCGCTGCCAGCTGCA
88	core		CCAGTAGTTAAGCCCTTTTTAAGAAAAGCAAA

89	core		TGGCGAAGTTGGGACTTTCCG
90	core		CAGTGAGTGATGGTGGTTCCGAAAACCGTCTATCACGATTTA
91	core		AAATCAAAGAGAATAACATAACTGAACACAGT
92	core		CTGTATGACAACTAGTGTCGA
93	core		ATCATAAATAGCGAGAGGCTTAGCAAAGCGGATTGTTCAAAT
94	core		TTGAGTAATTTGAGGATTTAGCTGAAAGGCGCGAAAGATAAA
95	core		ATAAGAATAAACACCGCTCAA
96	core		CGTTGTAATTCACCTTCTGACAAGTATTTTAA
97	core		AACCGCCTCATAATTCGGCATAGCAGCA
98	core		AAATAGGTCACGTTGGTAGCGAGTCGCGTCTAATTCGC
99	core		CAGTATAGCCTGTTTATCAACCCCATCC
100	core		TTGCACCTGAAAATAGCAGCCAGAGGGTCATCGATTTTCGGT
101	core		CGTCGGAAATGGGACCTGTCGGGGGAGA
102	core		AAGAAACTAGAAGATTGCGCAACTAGGG
103	core		CCAGAACCTGGCTCATTATACAATTACG
104	core		ACGGGTAATAAATTAAGGAATTGCGAATAGTA
105	core		CCACGCTGGCCGATTCAAACTATCGGCCCGCT
106	core		GCCTTCACCGAAAGCCTCCGCTCACGCCAGC
107	core		CAGCATTAAAGACAACCGTCAAAAATCA
108	core		ACATCGGAAATTATTTGCACGTAAAAGT
109	core		CAACGGTCGCTGAGGCTTGATACCTATCGGTTTATCAGATCT
110	core		AAATCGTACAGTACATAAATCAGATGAA
111	core		TTAACACACAGGAACACTTGCCTGAGTATTTG
112	core		AGGCATAAGAAGTTTTGCCAGACCCTGA
113	core		GACGACATTCACCAGAGATTAAAGCCTATTAACCA
114	core		AGCTGCTCGTTAATAAAACGAGAATACC
115	core		CTTAGAGTACCTTTTAAACAGCTGCGGAGATTTAGACTA
116	core		CACCCTCTAATTAGCGTTTGCTACATAC
117	core		GAACCGAAAATTGGGCTTGAGTACCTTATGCGATTCAACACT
118	core		GCAAGGCAGATAACATAGCCGAACAAAGTGGCAACGGGA
119	core		ATGAAACAATTGAGAAGGAAACCGAGGATAGA
120	core		GGATGTGAAATTGTTATGGGGTGCACAGTAT
121	core		GGCTTGCGACGTTGGGAAGAACAGATAC
122	core		TAAATGCCTACTAATAGTAGTTTTCATT
123	core		TGCCGTCTGCCTATTTCGGAACCAGAATGGAAAGCCCACCAGAAC
124	core		TGACCATAGCAAAAGGGAGAACAAC
125	core		CGAGCCAGACGTTAATAATTTGTATCA
126	core		GCTCAGTTTCTGAAACATGAAACAAATAAATCCTCCCGCCGC
127	core		AGACGCTACATCAAGAAAACACTTTGAA
128	core		AGTACTGACCAATCCGCGAAGTTTAAGACAG
129	core		GATTCCTGTTACGGGCAGTGAGCTTTTCCTGTGTGCTG
130	core		GGTATTAAGGAATCATTACCGAACGCTA
131	core		GTTCATCAAATAAAACGCGACTCTAGAGGATCGGG
132	core		AGCCTTTAATTGGATAGTTGAACCGCCACCCTCATAGGTG
133	core		ACAGAGGCCTGAGATTCTTTGATTAGTAATGG
134	core		AACGAGATCAGGATTAGAGAGCTTAATT
135	core		TACCAAGTTATACTTCTGAATCACCAGA
136	core		CAGTAGGTGTTCAGCTAATGCGTAGAAA

137	core		AGGATGACCATAGACTGACTAATGAAATCTACATTCAGCAGGCGCG TAC
138	core		TTTCAACCAAGGCAAAGAATTTAGATAC
139	core		TTGAAATTAAGATAGCTTAACTAT
140	core		CTATTATCGAGCTTCAAAGCGTATGCAA
141	core		CAGGGTGCAAAATCCCTTATAGACTCCAACGTCAAAAGCCGG
142	core		GAGCTTGTTAATGCGCCGCTAATTTTAGCGCCTGCTGCTGAA
143	core		CGAACGTTAACCACCACACCCCCAGAATTGAG
144	core		GTGTGATAAATAAGTGAGAAT
145	core		GCTATATAGCATTAACCCTCAGAGA
146	core		AGGAGAGCCGGCAGTCTTGCCCCCGAGAGGGAGGG
147	core		CGGCCTCCAGCCAGAGGGCGAGCCCCAA
148	core		CCAAAACAAAATAGGCTGGCTGACGTAACAA
149	core		GGCGGTTAGAATAGCCCGAGAAGTCCACTATTAAAAAGGAAG
150	core		ATAAAGGTTACCAGCGCTAATTCAAAAACAGC
151	core		ATTGCCCCCAGCAGGCGAAAAGGCCCACTACGTGACGGAACC
152	core		TTTTAAAACATAACAGTAATGGAACGCTATTAGAACGC
153	core		AATTGGGTAACGCCAGGCTGTAGCCAGCTAGTAAACGT
154	edge		TTACCCAGAACAACATTATTACAGGTTTTTTTTTTTTTTTT
155	edge		TTTTTTTTTTTTTTTTAATAAGAGAATA
156	edge		TTTTTTTTTTTTTTTCCAGTTTGGGAGCGGGCTTTTTTTTTTTTTTTT
157	edge		GGTTGAGGCAGGTCAGTTTTTTTTTTTTTTT
158	edge		TTTTTTTTTTTTTTTGATTAAGACTCCTTATCCAAAAGGAAT
159	edge		TTTTTTTTTTTTTTTTCTTCGCTATTACAATT
160	edge		TTTTTTTTTTTTTTTCTTGCGGGAGAAGCGCATTTTTTTTTTTTTTTT
161	edge		TTTTTTTTTTTTTTGGGAATTAGAGAAACAATGAATTTTTTTTTTTTT TT
162	edge		TCAGACTGACAGAATCAAGTTTGTTTTTTTTTTTTTTT
163	edge		TTTTTTTTTTTTTTTTGGTCGAGGTGCCGTAAAGCAGCACGT
164	edge		TTTTTTTTTTTTTTTTAATCATTTACCAGACTTTTTTTTTTTTTTTTT
165	edge		TTTTTTTTTTTTTCATTCTGGCCAAATTCGACAACTCTTTTTTTTTTTTT T
166	edge		TTTTTTTTTTTTTTTACCGGATATTCA
167	edge		TTTTTTTTTTTTTTTTAGACGGGAAACTGGCATTTTTTTTTTTTTTTT
168	edge		TTTTTTTTTTTTTTTCAGCAAGCGGTCCACGCTGCCCAAAT
169	edge		CTGAGAGAGTTGTTTTTTTTTTTTTTT
170	edge		CAATGACAACAACCATTTTTTTTTTTTTTTT
171	edge		TTTTTTTTTTTTTTTGAGAGATCTACAAGGAGAGG
172	edge		TCACCAGTACAAACTATTTTTTTTTTTTTTT
173	edge		TTTTTTTTTTTTTGGCAATTCATCAAATTATTCATTTTTTTTTTTTTTT T
174	edge		TAAAGTTACCGCACTCATCGAGAACTTTTTTTTTTTTTTT
175	edge		TTTTTTTTTTTTTTTCACCCTCAGAACCGCC
176	edge		TTTTTTTTTTTTTAGGTTTAACGTCAATATATGTGAGTTTTTTTTTTTT T
177	edge		CCACACAACATACGTTTTTTTTTTTTT
178	edge		TTTTTTTTTTTTTTTGCTAGGGCGAGTAAAAGATTTTTTTTTTTTTTT
179	edge		TTTTTTTTTTTTTTTAGTTGATTCCCAATTCTGCGAACCTCA
180	edge		TTATTTAGAGCCTAATTTGCCAGTTTTTTTTTTTTTTTTT
181	edge		TTTTTTTTTTTTTTTACGGCGGAT
182	edge		TTTTTTTTTTTTTTTATATGCGTTAAGTCCTGATTTTTTTTTTTTTTT

183	edge		TTTTTTTTTTTTTTTACGATTGGCCTTGATA
184	edge		TTTTTTTTTTTTTTTCAACGCCTGTAGCATT
185	edge		TTTTTTTTTTTTTTTTGGCTTTGAGCCGGAACGATTTTTTTTTTTTTTT
186	edge		TTTTTTTTTTTTTTTAAGCAAGCCGTTT
187	edge		TTTTTTTTTTTTTATGTGTAGGTAAGTACCCCGGTTGTTTTTTTTTTTT T
188	edge		ATCGTCATAAATATTCATTTTTTTTTTTTTTTT
189	edge		TTTTTTTTTTTTTTTTGTTAATTTCATCT
190	edge		TTTTTTTTTTTTTGTATTAAATCCTGCGTAGATTTTCTTTTTTTTTTTT T
191	edge		GCCATATAAGAGCAAGCCAGCCCGACTTGAGCCATGGTT
192	edge		GTAGCTAGTACCAAAAACATTCATAAAGCTAAATCGGTTTTTTTTTT TTT
193	edge		ATAACGTGCTTTTTTTTTTTTTTTTT
194	edge		TTTTTTTTTTTTTTTAAAATACCGAACGAACCACCAGTGAGAATTAA C
195	edge		TTTTTTTTTTTTTTTACAAAATAAACA
196	edge		TTTTTTTTTTTTTTTTACAAGAAAAACCTCCCGATTTTTTTTTTTTTTT
197	edge		TTTTTTTTTTTTTTTTGACGATAAAAAGATTAAGTTTTTTTTTTTTTTT
198	edge		TTTTTTTTTTTTTCAATTACCTGAGTATCAAAATCATTTTTTTTTTTTT T
199	edge		GGTACGGCCAGTGCCAAGCTTTTTTTTTTTTTTT
200	edge		TTTTTTTTTTTTTGAATAACCTTGAAATATATTTATTTTTTTTTTTT T
201	edge		CACTAAAACACTTTTTTTTTTTTTTT
202	edge		TTTTTTTTTTTTTTTTAACCAATATGGGAACAATTTTTTTTTTTTTTT
203	edge		TACGTCACAATCAATAGAATTTTTTTTTTTTTTT
204	edge		TTTTTTTTTTTTTTTAGAAAGATTCATCAGTTGA
205	edge		TTTTTTTTTTTTTGTGGCATCAATTAATGCCTGAGTATTTTTTTTTTTT T
206	edge		TTTTTTTTTTTTTTTTTTGCATGCCTGCATTAATTTTTTTTTTTTTTTT
207	edge		CCAGCGAAAGAGTAATCTTGACAAGATTTTTTTTTTTTTTT
208	edge		TTTTTTTTTTTTTTTGAATCCCCCTCAAATGCTT
209	edge		AGAGGCTGAGACTCCTTTTTTTTTTTTTTT
210	edge		ACAAACACAGAGATACATCGCCATTATTTTTTTTTTTTTTT
211	edge		TTTTTTTTTTTTTTTCAAGAGAAGGATTAGG
212	edge		TTTTTTTTTTTTTGAATTGAGGAAGTTATCAGATGATTTTTTTTTTTTT T
213	edge		CAGAACAATATTTTTTTTTTTTTTTTT
214	edge		TTTTTTTTTTTTTAGCCGGAAGCATAAAGTGTCCTGGCC
215	edge		TGACCGTTTCTCCGGGAACGCAAATCAGCTCATTTTTTTTTTTTTTT TT
216	edge		TTTTTTTTTTTTTTTGGTAATAAGTTTTAAC
217	edge		TTTTTTTTTTTTTTGTCTGTCCATAATAAAAGGGATTTTTTTTTTTTT T
218	edge		TTTTTTTTTTTTTTTCCTCGTTAGAATCAGAGCGTAATATC
219	edge		AATTGCTCCTTTTGATAAGTTTTTTTTTTTTTTT
220	edge		CATCGGACAGCCCTGCTAAACAACTTTCAACAGTTTTTTTTTTTTTTT
221	edge		TTTTTTTTTTTTTTTAACCGCCTCCCTCAGACCAGAGC
222	edge		TCTGACAGAGGCATTTTCGAGCCAGTTTTTTTTTTTTTTT
223	edge		TTTTTTTTTTTTTTTTTTCAGCGGAGTTCCATGTCATAAGG
224	edge		TTTTTTTTTTTTTTTCGCCCACGCATAACCG
225	edge		AATTACTTAGGACTAAATAGCAACGGCTACAGATTTTTTTTTTTTTT T

226	edge		CAAGTTTTTGGTTTTTTTTTTTTTTT
227	edge		TTTTTTTTTTTTTTTCCTTTAGCGCACCACCGGTTTTTTTTTTTTTTT
228	edge		TTTTTTTTTTTTTTTGAATCGGCCGAGTGTTGTTTTTTTTTTTTTTT
229	edge		TTTTTTTTTTTTTTTCATCTTTGACCC
230	edge		TTTTTTTTTTTTTTTATAATCAGAAAATCGGTGCGGCCTTTTTTTTTTTTT TT
231	edge		GATACAGGAGTGTACTTTTTTTTTTTTTTT
232	edge		TTTTTTTTTTTTTTTGGCGCAGACAATTTCAACTTTTTTTTTTTTTTT
233	edge		GGAGGTTTAGTACCGCTTTTTTTTTTTTTTT
234	edge		TTTTTTTTTTTTTTTACCGCCAGCCATAACAGTTGAAAGTTTTTTTTTTTTT TT
235	edge		TTTTTTTTTTTTTTTATAGCAATAGCT
236	Key handle		AATAAGTTTTGCAAGCCCAATAGGGGATAAGTATCGGATGACTATA CT
237	handles		ACATAGCTTACATTTAACAATAATAACGTTGTGCTACTCCAGTTC
238	handles		CCTTTTTGAATGGCGTCAGTATTGTGCTACTCCAGTTC
239	handles		CGTAACCAATTCATCAACATTTTGTGCTACTCCAGTTC
240	handles		CACCAACCGATATTCATTACCATTATTGTGCTACTCCAGTTC
241	handles		CCACCCTCATTTTCTTGATATTTGTGCTACTCCAGTTC
242	handles		AACTTTGAAAGAGGAGAAACATTGTGCTACTCCAGTTC
243	handles		CAAGGCGCGCCATTGCCGGAATTGTGCTACTCCAGTTC
244	handles		CATAGCCCCCTTAAGTCACCATTGTGCTACTCCAGTTC
245	handles		TTTCCCTGAATTACCTTTTTTACCTTTTTTGTGCTACTCCAGTTC
246	handles		AACGGTGTACAGACTGAATAATTGTGCTACTCCAGTTC
247	handles		GATTCGCGGGTTAGAACCTACCATTTTGTTGTGCTACTCCAGTTC
248	guides		AGAGTAGGATTTCGCCAACATGTTTTAAAAACC
249	guides		ACGGTGACCTGTTTAGCTGAATATAATGCCAAC
250	guides		CGTAGCAATTTAGTTCTAAAGTACGGTGTTTTA
251	guides		GCTTAATGCGTTAAATGTAAATGCTGATCTTGAAATGAGCGTT
252	guides		AAGCCAACGGAATCTAGGTTGGGTTATATAGATTAAGCAACTG
253	guides		TTTAACAACCGACCCAATCGCAAGACAAAATTAATCTCACTGC
254	guides		TTTAGGCCTAAATTGAGAAAACTTTTTCCTTCTGTTCCTAGAT
255	guide removal		GGTTTTTAAAACATGTTGGCGAAATCCTACTCT
256	guide removal		GTTGGCATTATATTCAGCTAAACAGGTCACCGT
257	guide removal		TAAAACACCGTACTTTAGAACTAAATTGCTACG
258	guide removal		AACGCTCATTTCAAGATCAGCATTTACATTTAACGCATTAAGC
259	guide removal		CAGTTGCTTAATCTATATAACCCAACCTAGATTCCGTTGGCTT
260	guide removal		GCAGTGAGATTAATTTTGTCTTGCGATTGGGTCGGTTGTTAAA
261	guide removal		ATCTAGGAACAGAAGGAAAAAGTTTTCTCAATTTAGGCCTAAA
262	gates	P_apt1	TGGGGCGCGAGCTGAAAAGTACTCAGGGCACTGCAAGCAATTGTGG TCCCAATGGGCTGAGTA
263	gates	P_com1	TGATGAGCGTGGATGATACTCAGCCCATTGGGTTTTTTTTTTTTTTTT TTTTTTTTTTTTTAGGTCATTTTTGCGGATGG
264	gates	P_apt2	ATACAAAAAGCCTGTTTAGTATCTACTCAGGGCACTGCAAGCAATT GTGGTCCCAATGGGCTGAGTA
265	gates	P_com2	TACTCAGCCCATTGGGTTTTTTTTTTTTTTTTTTTTTTTTTTTTTTAGGTC TGAGAGACTACCTT
266	gates	V_apt1	TGGGGCGCGAGCTGAAAAGATACCAGTCTATTCAATTGGGCCCGTC CGTATGGTGGGTGTGCT
267	gates	V_com1	AGCACACCCACCATACTTTTTTTTTTTTTTTTTTTTTTTTTTTTTTTAGGTC ATTTTTGCGGATGG
268	gates	V_apt2	ATACAAAAAGCCTGTTTAGTATCATACCAGTCTATTCAATTGGGCCC GTCCGTATGGTGGGTGTGCT
269	gates	V_com2	TGATGAGCATGGCATCAGCACACCCACCATACTTTTTTTTTTTTTTT

			TTTTTTTTTTTTAGGTCTGAGAGACTACCTT
270	gates	P_apt3	TGGGGCGCGAGCTGAAAAGTACTCAGGGCACTGCAAGCAATTGTGG TCCCAATGGGCTGAGTA
271	gates	P_com3	ACCTAGTGTACTCAGCCCATTGGGTTTTTTTTTTTTTTTTTTTTTTTTT TTTAGGTCATTTTTGCGGATGG
272	gates	V_apt3	ATACAAAAAGCCTGTTTAGTATCATACCAGTCTATTCAATTGGGCCC GTCCGTATGGTGGGTGTGCT
273	gates	V_com3	TACGGAGTAGCACACCCACCATACTTTTTTTTTTTTTTTTTTTTTTTTT TTTAGGTCTGAGAGACTACCTT
274	gates	P1_Mag_key	AAGTATGGTGGGTGTGCTGATGCCATTTTTTAGTATAGTCATCCGAT A
275	gates	P2_Ora_key	AACCCAATGGGCTGAGTATCATCCACTTTTTAGTATAGTCATCCGAT A
276	gates	P3_Red_key	AAGTATGGTGGGTGTGCTACTCCGTATTTTTAGTATAGTCATCCGAT A
277	gates	N_clasp1	CCCAATGGGCTGAGTATCATCCACGCTCATCATTTTTGAACTGGAGT AGCAC
278	gates	N_clasp2	GTATGGTGGGTGTGCTGATGCCATGCTCATCATTTTTGAACTGGAGT AGCAC

Gate and payload configuration per robot type:

E: P_apt1/P_com1 + V_apt2/V_com2 + antibody fragment
P1: P_apt1/P_com1 + P_apt2/P_com2 + magenta key
P2: V_apt1/V_com1 + V_apt2/V_com2 + orange key
N: P_apt2/P_com2 + V_apt1/V_com1 + clasps
F: P_apt3/P_com3 + V_apt3/V_com3 + drug
P3: P_apt1/P_com1 + P_apt2/P_com2 + red key

Robot preparation:

Robots were initially produced by mixing M13mp18 ssDNA as scaffold strand (NEB, N4040, final concentration of 20 nM) and staple strands (final concentrations of 200 nM of each strand), purchased from Integrated DNA Technologies. Buffer and salts of solution included 5mM Tris, 1mM EDTA (pH 8.0 at 20 ^{o}C) and 10 mM $MgCl_2$. The mixture was subjected to a thermal-annealing ramp for folding. Initially the following program was used: 80 ^{o}C to 60 ^{o}C at 2 min/^{o}C, 60 ^{o}C to 20 ^{o}C at 150 min/^{o}C. Later, a robust folding condition screening was carried out and folding sequence was considerably optimized (**Supplementary Fig. 4**).

Two proteins – human platelet-derived growth factor BB (PDGF-BB) and human vascular endothelial derived growth factor 165 ($VEGF_{165}$) – were used as cues, and the DNA aptamers binding them[1,2] (41t in the case of PDGF, SL12 in the case of VEGF) were used as gates. Typical robot mixture contained 0.1 pmol of the effector robot, and 0.2 pmol or more of each regulator robot, as described below.
It is important to note that we used exogenous, human-origin cues as a proof of principle rather than endogenous cues, to which generating stable sensing strands that function in biological conditions proved technically challenging. However, we continue to generate DNA aptamers for a variety of murine cues to demonstrate the scalability of our system using endogenous cues in a mammal. In future designs, endogenous DNA or RNA cues could be used rather than proteins or other molecules that require aptamer-based sensing, which would likely contribute to scalability and performance, however this concept needs to be investigated further.

Folding Duration [hrs]	30	30	30	30	30	30	30	60	60	60	60	60	60	60	30	60
Staples : Scaffold ratio	10	10	10	10	5	5	5	10	10	10	5	5	5	5	5	5
Tris-HCl [mM]	10	10	5	5	10	10	5	10	10	5	5	10	5	5	5	10
NaCl [mM]	0	5	0	5	0	5	5	0	5	0	5	0	0	5	0	5

M Scaffold 1 2 3 4 5 6 7 8 9 10 11 12 13 14 15 16

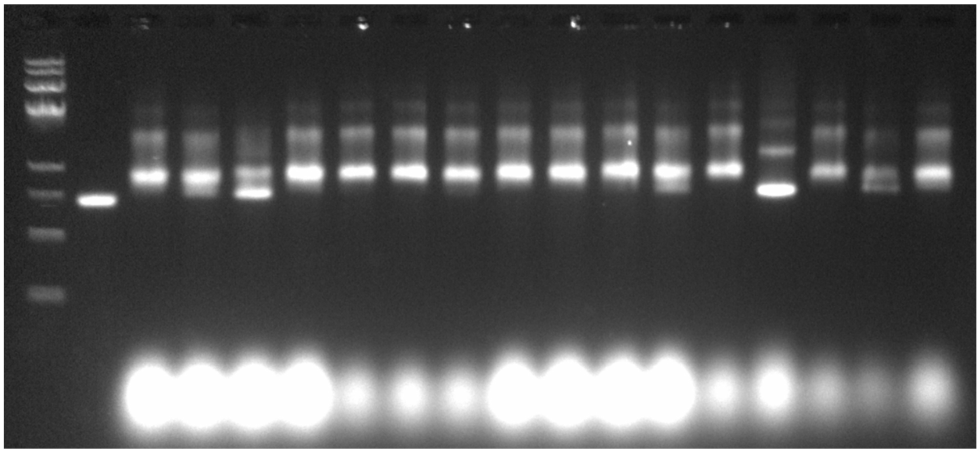

Supplementary Fig. 4: Agarose-gel analysis of folding conditions. 'Folding Duration' refers to either a 60-hours long fold (80-60 ^{o}C at 5 min/^{o}C, 60-10^{o}C at 75 min/^{o}C) or a 30-hours long fold (80-60 ^{o}C at 5 min/^{o}C, 60-10^{o}C at 50 min/^{o}C). 'Staples/Scaffold' refers to the excess molar ratio of each staple to scaffold DNA. Either a 10- or a 5- staples molar excess ratios were used. Scaffold was used at 20 nM final concentration. EDTA was used at a 1 mM final concentration. $MgCl_2$ concentration was 10 mM. Folding volume was 50 μL. Lanes 3 and 13 indicate particularly good folding of robots.

Purification of folded robots:

After folding, excess staples were removed by centrifugal filtration using Amicon Ultra-0.5 mL 100K centrifugal filters (Millipore). Folding buffer was added to reach a total volume of 500 µL, after which samples were centrifuged at 12,000 g for 10min. this was repeated three times as previously described. DNA concentration was measured by spectrophotometer (Thermo Sci. NanoDrop 2000c).

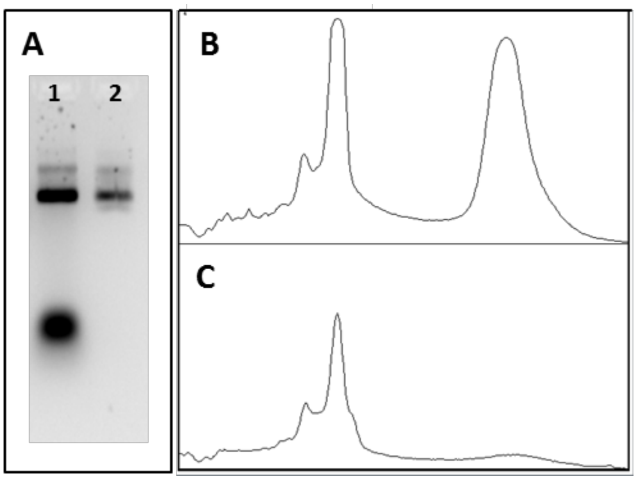

Supplementary Fig. 5: Nanorobot excess staples purification. **A)** Gel migration pattern of nanorobots before removal of excess staples (lane 1) and after (lane 2). **B)** histograms of lane 1 in **A**. **C)** histogram of lane 2 in **A**. histograms were generated by ImageJ 1.42q software.

Gel purification of folded samples:

Leading monomer bands were visualized on a UV table and excised from a 1.5%-2% agarose gel (running buffer is 0.5X TBE supplemented with 10 mM $MgCl_2$), frozen at -20 ^{o}C for 5 min, chopped to small pieces and centrifuged at 13,000 g for 3 min inside a Quantum Prep Freeze N' Squeeze DNA Gel Extraction spin column (Bio-Rad). Recovered solution was measured for DNA concentration by spectrophotometer (Thermo Sci. NanoDrop 2000c) and prepared for imaging by transmission electron microscopy (TEM).

TEM negative-stain:

Negative staining of robots was done as previously described[3]. Briefly, 5 µL of 0.5 M NaOH are added to a pre-made frozen aliquot of 100 µL 2% uranyl formate solution (Polysciences, 24762) followed by rigorous vortexing for 3 minutes, after which solution is centrifuged at 18,000 g for 5 minutes and precipitate is removed. Robot samples at 1-5 nM concentration are loaded onto a TEM Grid (Science Services, EFCF400-Cu-50) immediately after glow-discharge treatment (Emitech K100X), followed by two consecutive washes with 0.1% uranyl formate solution. During the third wash the grid is incubated with uranyl formate solution for 30 seconds. Samples are visualized using a TEM microscope (JEM-1400, JEOL) an hour to one week after negative staining.

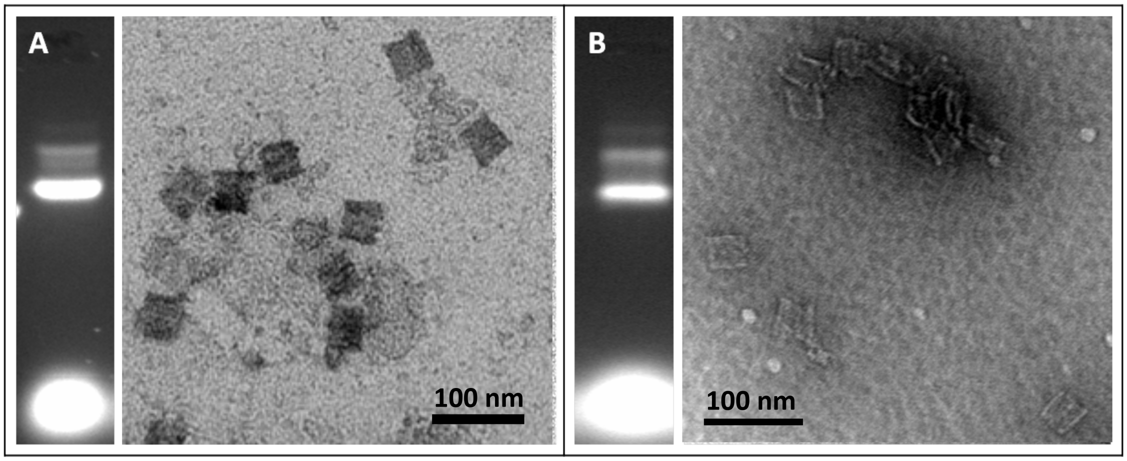

Supplementary Fig. 6: Agarose-gel analysis and TEM photos of different folding durations. Both samples were folded at 20 nM scaffold concentration, 200 nM staples concentration, 1X TAE, 10 mM $MgCl_2$. After folding, excess staples were removed using micon Ultra–0.5 mL 100K centrifugal filters (Millipore). **A)** Folding duration is 80-60 ^oC at 2 min/^oC and 60-10 ^oC at 150 min/^oC. **B)** Folding duration is 80-60 ^oC at 5 min/^oC, 60-10 ^oC at 75 min/^oC.

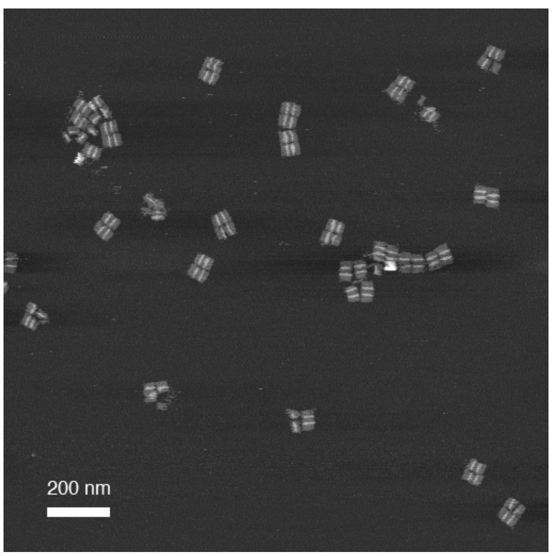

Supplementary Fig. 7: AFM image of folded robots. Robots after folding and staple removal were dispensed on a newly cleaved mica surface at a concentration of 5 nM in TAE containing 10 mM Mg^{2+}. AFM images were acquired on a Veeco Multimode V atomic force microscope at ScanAsyst mode in fluid as previously described. Bar = 200 nm.

Antibody payload preparation:

Antibodies were digested using a commercial kit (Thermo) with immobilized ficin in mouse IgG digestion buffer with 25 mM cysteine by shaking at a 37 ^{o}C water bath for 4 hours. Antibody Fab' fragments were purified by centrifugal filtration (Amicon, 10K MWCO Millipore) and evaluated by spectrophotometer (Thermo Sci. NanoDrop 2000c). Fab' fragments were buffer-exchanged into 0.05 M sodium borate buffer, pH 8.5, and incubated with DyLight Amine-Reactive Dye (Thermo) for 1 hour at room temperature on a rotary shaker. Excess dye was thoroughly removed using Amicon 10K MWCO (Millipore). Fab' fragments were incubated for 1 minute with 5'-amine-modified linker oligonucleotide (5AmMC6/GAACTGGAGTAGCAC, Integrated DNA Technologies) at a molar ratio of 1 to 10, in a 0.1 M MES-buffered saline, pH 4.7 (Pierce #28390). EDC (Thermo, #22980) was added at a molar ratio of 5000 to 1 Fab' fragment and incubated at room temperature for 1 hour on a rotary shaker. Afterwards, Tris was added to a final concentration of 10 mM and solution was filtered via Amicon column 30K MWCO (Millipore).

Loading of robot with antibody:

Oligonucleotide-Fab' concentration was evaluated via absorption at 260 and 280 nm. Loading was performed for 2 hours on a rotary shaker at room temperature in folding buffer (10 mM $MgCl_2$ in 1X TAE) at a 2-fold molar excess of payloads to loading sites. Finally, loaded robots were cleaned by centrifugal filtration with a 100K MWCO Amicon column (Millipore) as described above.

Supplementary Note 2: Robot collision programming

System design:
Cue-driven collisions between robots were based on toehold-mediated strand displacement reactions. The basic design enabling collisions between DNA strands extending from E, P, and N robots was based on a 3-level interaction: the first level is the interaction of the cue itself (e.g. PDGF or VEGF in this study) with the sensing strands of the gates of all robots (E, P, and N). Alternatively, the E gates can also interact with either P or N as described in **Supplementary Fig. 8-9** below.

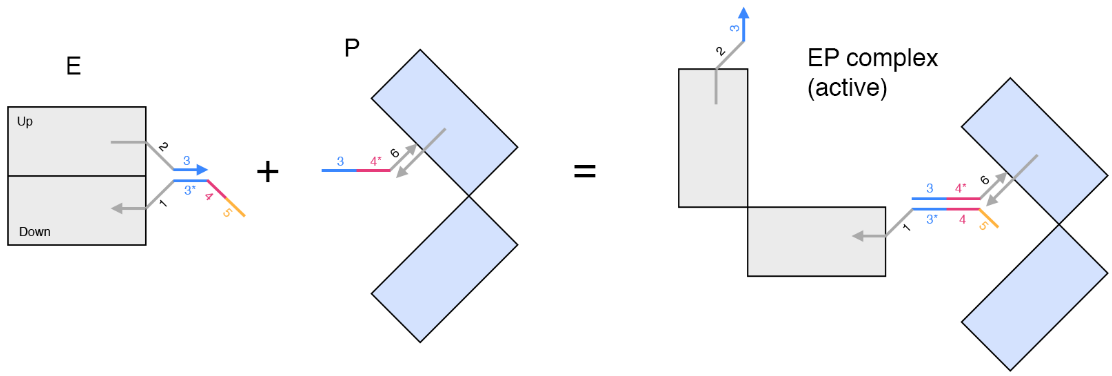

Supplementary Fig. 8: Collision between E and P. Robots are depicted here from a side view schematically as rectangles revolving around a vertical axis. The E gate complementary strand contains four regions (from 5' to 3'): 5 (toehold for collision with N), 4 (toehold for collision with P), 3* (partially complements with the aptamer), and 1 (anchors the gate to the robot chassis). The sensing strand contains two regions (from 5' to 3'): 2 (anchors the gate to the robot chassis) and 3 (the aptamer). The key loaded into P contains 3 regions (from 5' to 3'): 3 (portion of the sensing strand which only appear identical in this scheme), 4* (hybridizes with toehold 4), and 6 (loading sequence to robot).

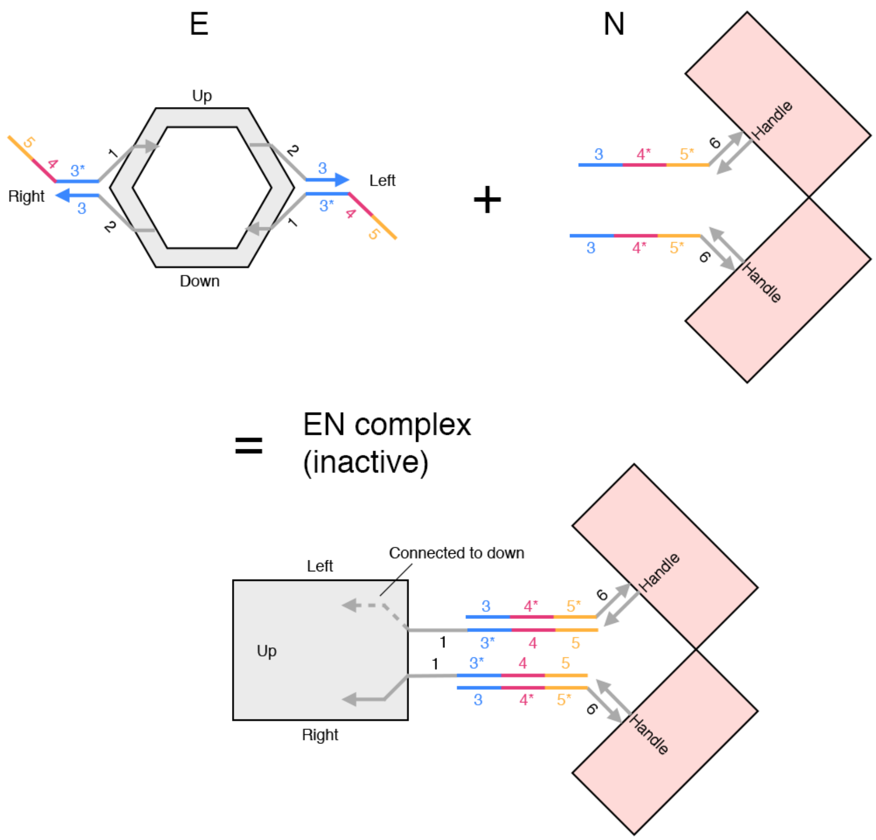

Supplementary Fig. 9: Collision between E and N. E robots are shown here first from a front view with the virtual sides stated for proper orientation. The arms (clasps) extending from N include 4 regions (from 5' to 3'): 3 (portion of the sensing strand which only appear identical in this scheme), 4* (hybridizes with toehold 4), 5* (hybridizes with toehold 5), and 6 (loading sequence to robot, which is not identical to the loading sequence in **Supplementary Fig. 8**). Multiple arms extending from N clasp the two gates of E. Since these are located on opposite sides of the robot (up and down), the result is inability of E to open properly.

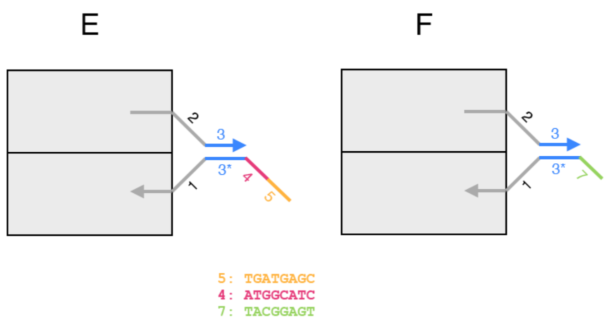

Supplementary Fig. 10: Structural basis for differential keying of E and F robots. E and F consist of different regions dictating collisions with P and N. P1 and P2 robots key E by interacting with region 4 on the E gate **(Supplementary Fig. 8)**. N robots close E by interacting with region 5 **(Supplementary Fig. 9)**. Since F robots contain neither region

4 nor 5, robots P1, P2 and N cannot interact with it. However, P3 keys F by interacting with region 7, which is also why it cannot key E.
It is important to note that the N gate complementary strands lack regions 5 and 4, so the N clasp arms cannot hybridize with them and inactivate N itself.

Based on this basic design, collision-mediating sequences were chosen and the resulting systems EP, EN and EPN were modeled and prototyped in visual DSD (vDSD)[20]. The sequences were then altered as necessary to achieve the desired performance and kinetics **(Supplementary Fig. 11)**.

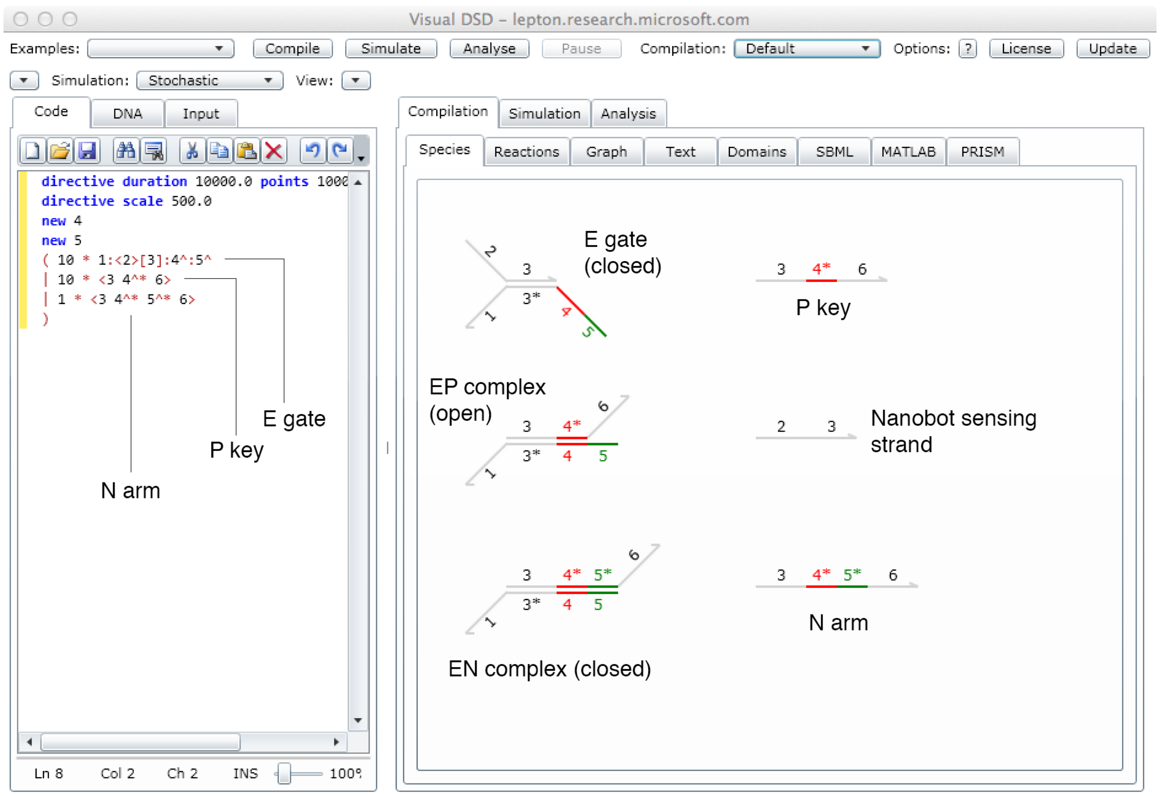

Supplementary Fig. 11: Modeling the robot collision system in vDSD. Compiling the code written in the left window generates all the DNA strands taking part in our collision system, with tunable concentrations (numbers before the asterisks in the three last lines of code). Note that E gate is abstracted in the code as a single line representing two strands, according to the vDSD syntax. The robot sensing strand is released from the E gate after EP complex formation.

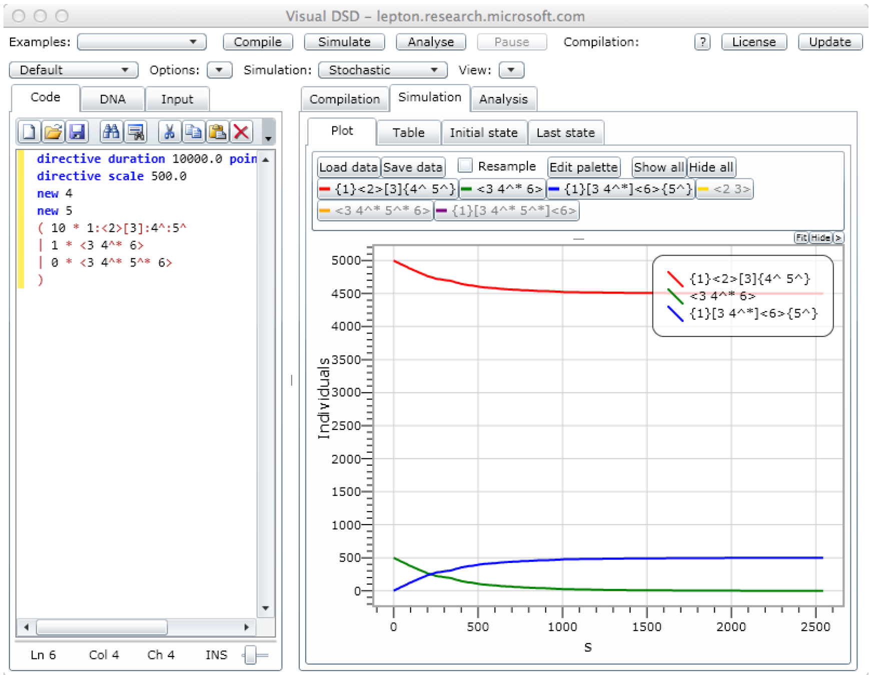
Visual DSD – lepton.research.microsoft.com
Examples:
Compile
Simulate
Analyse
Pause
Compilation:
License
Update
Default
Options:
Simulation:
Stochastic
View:
Code
DNA
Input
Compilation
Simulation
Analysis
Plot
Table
Initial state
Last state
directive duration 10000.0 poin
directive scale 500.0
new 4
new 5
(10 * 1:<2>[3]:4^:5^
| 1 * <3 4^* 6>
| 0 * <3 4^* 5^* 6>
)
Load data
Save data
Resample
Edit palette
Show all
Hide all
{1}<2>[3]{4^ 5^}
<3 4^* 6>
{1}[3 4^*]<6>{5^}
<2 3>
<3 4^* 5^* 6>
{1}[3 4^* 5^*]<6>
Individuals
s
Ln 6
Col 4
Ch 4
INS

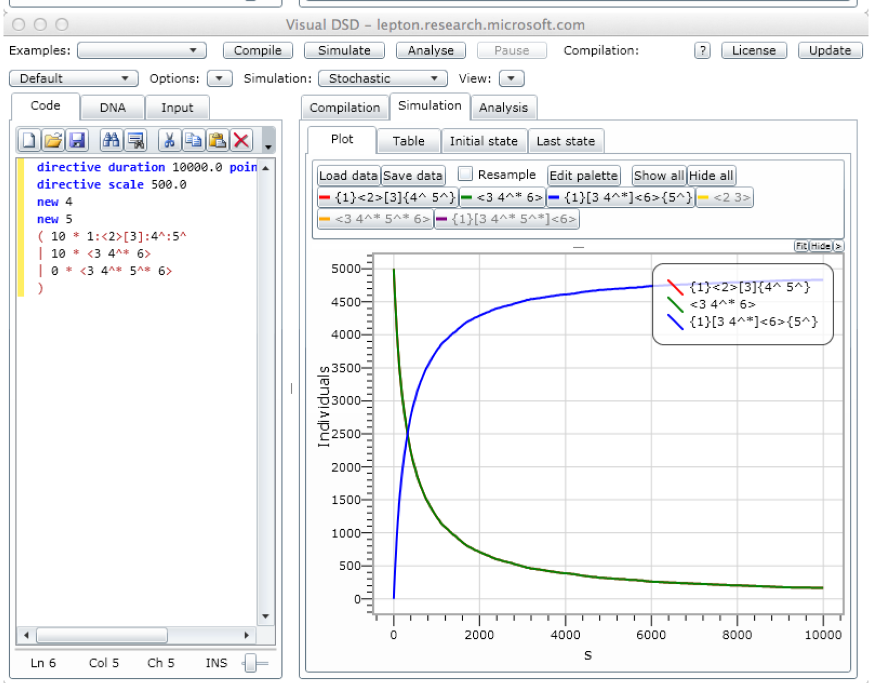
Visual DSD – lepton.research.microsoft.com
Examples:
Compile
Simulate
Analyse
Pause
Compilation:
License
Update
Default
Options:
Simulation:
Stochastic
View:
Code
DNA
Input
Compilation
Simulation
Analysis
Plot
Table
Initial state
Last state
directive duration 10000.0 poin
directive scale 500.0
new 4
new 5
(10 * 1:<2>[3]:4^:5^
| 10 * <3 4^* 6>
| 0 * <3 4^* 5^* 6>
)
Load data
Save data
Resample
Edit palette
Show all
Hide all
{1}<2>[3]{4^ 5^}
<3 4^* 6>
{1}[3 4^*]<6>{5^}
<2 3>
<3 4^* 5^* 6>
{1}[3 4^* 5^*]<6>
Individuals
s
Ln 6
Col 5
Ch 5
INS

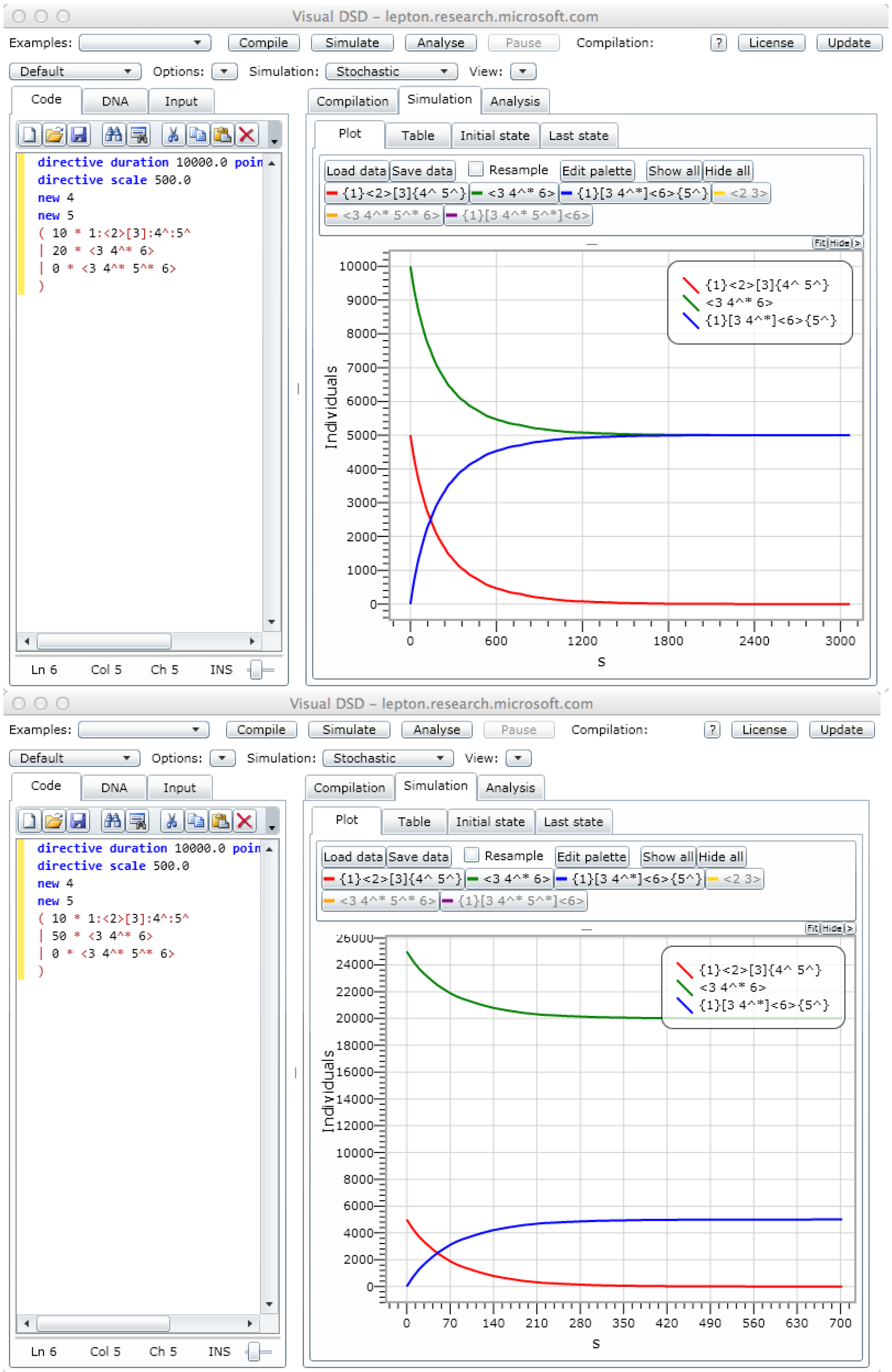

Supplementary Fig. 12: Simulated kinetics of the EP complex. E and P robots in varying stoichiometries – from 0.1 to 10 – were simulated in vDSD. The fastest reaction occurs when P is at a molar excess of 5 over E, consistently with the ex-vivo prototyping.

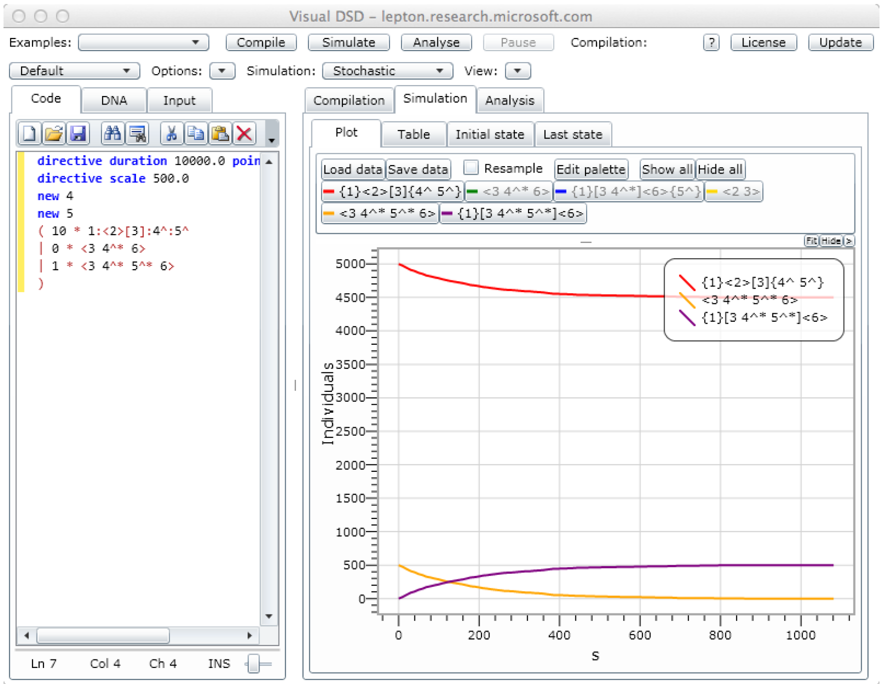

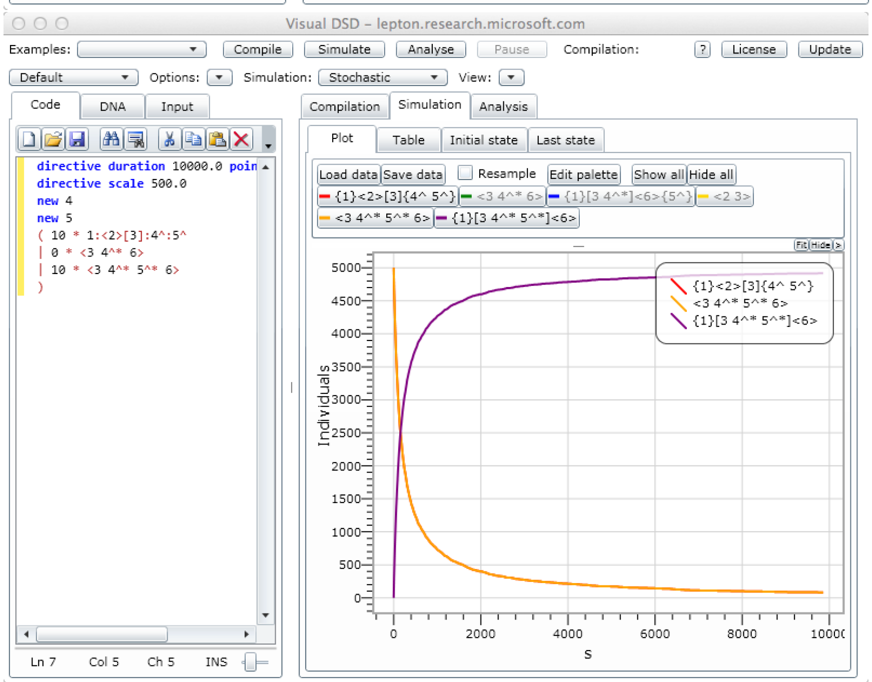

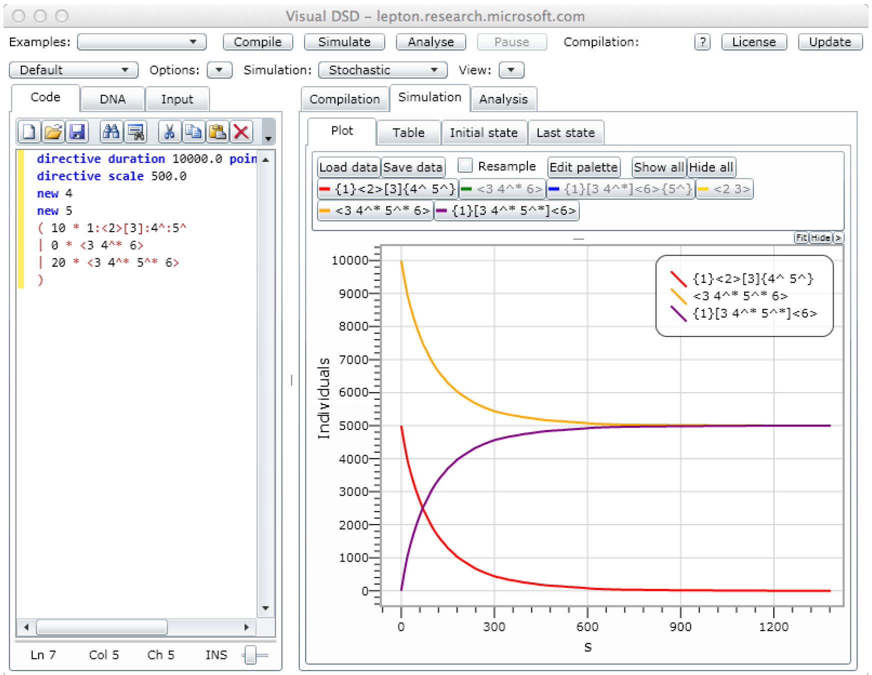
Visual DSD – lepton.research.microsoft.com
Examples:
Compile
Simulate
Analyse
Pause
Compilation:
?
License
Update
Default
Options:
Simulation:
Stochastic
View:
Code
DNA
Input
Compilation
Simulation
Analysis
Plot
Table
Initial state
Last state
directive duration 10000.0 poin
directive scale 500.0
new 4
new 5
(10 * 1:<2>[3]:4^:5^
| 0 * <3 4^* 6>
| 20 * <3 4^* 5^* 6>
)
Ln 7
Col 5
Ch 5
INS
Load data
Save data
Resample
Edit palette
Show all
Hide all
{1}<2>[3]{4^ 5^}
<3 4^* 6>
{1}[3 4^*]<6>{5^}
<2 3>
<3 4^* 5^* 6>
{1}[3 4^* 5^*]<6>
Individuals
s

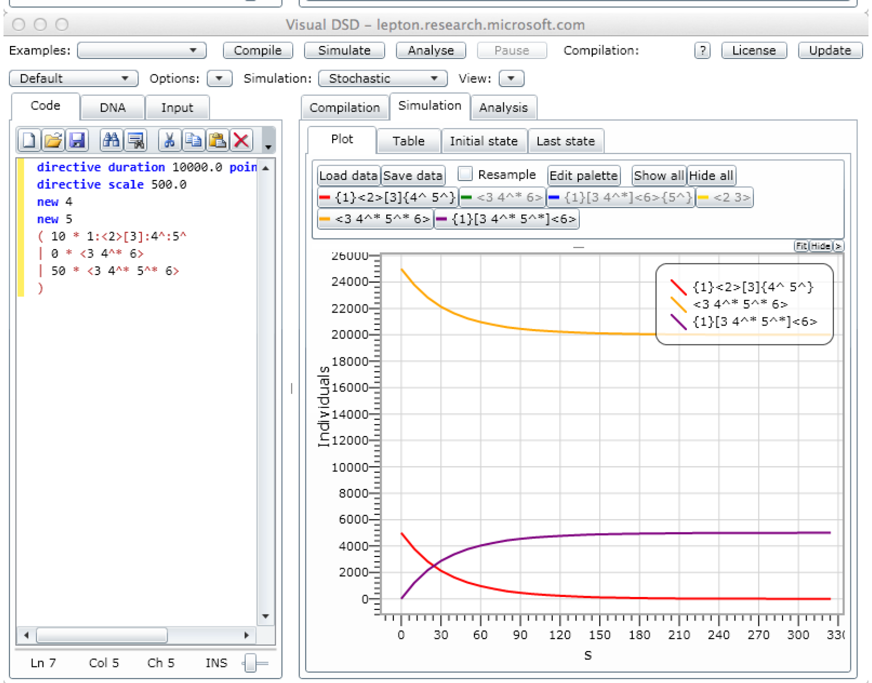
Visual DSD – lepton.research.microsoft.com
Examples:
Compile
Simulate
Analyse
Pause
Compilation:
?
License
Update
Default
Options:
Simulation:
Stochastic
View:
Code
DNA
Input
Compilation
Simulation
Analysis
Plot
Table
Initial state
Last state
directive duration 10000.0 poin
directive scale 500.0
new 4
new 5
(10 * 1:<2>[3]:4^:5^
| 0 * <3 4^* 6>
| 50 * <3 4^* 5^* 6>
)
Ln 7
Col 5
Ch 5
INS
Load data
Save data
Resample
Edit palette
Show all
Hide all
{1}<2>[3]{4^ 5^}
<3 4^* 6>
{1}[3 4^*]<6>{5^}
<2 3>
<3 4^* 5^* 6>
{1}[3 4^* 5^*]<6>
Individuals
s

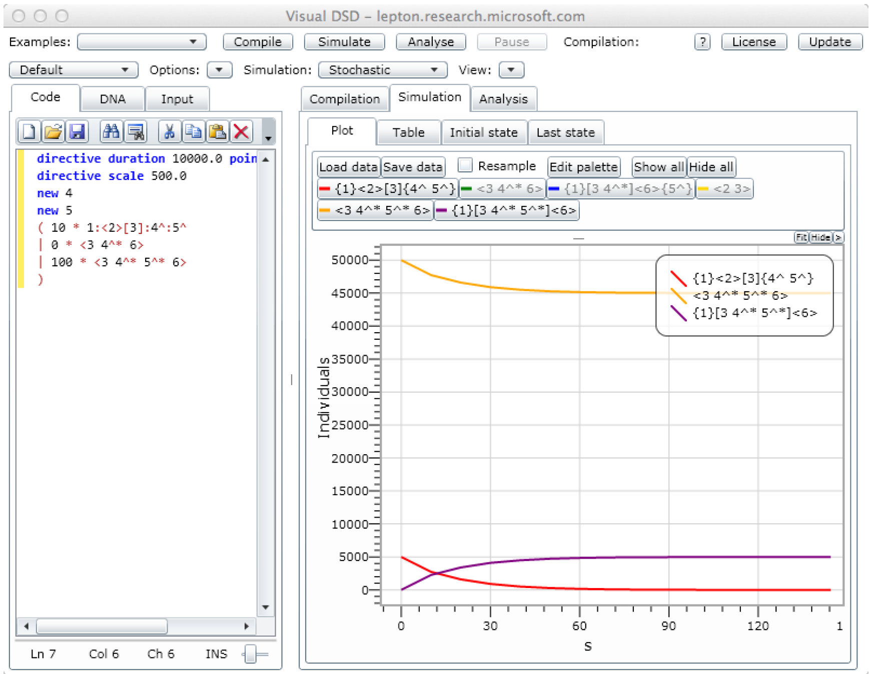

Supplementary Fig. 13: Simulated kinetics of the EN complex.

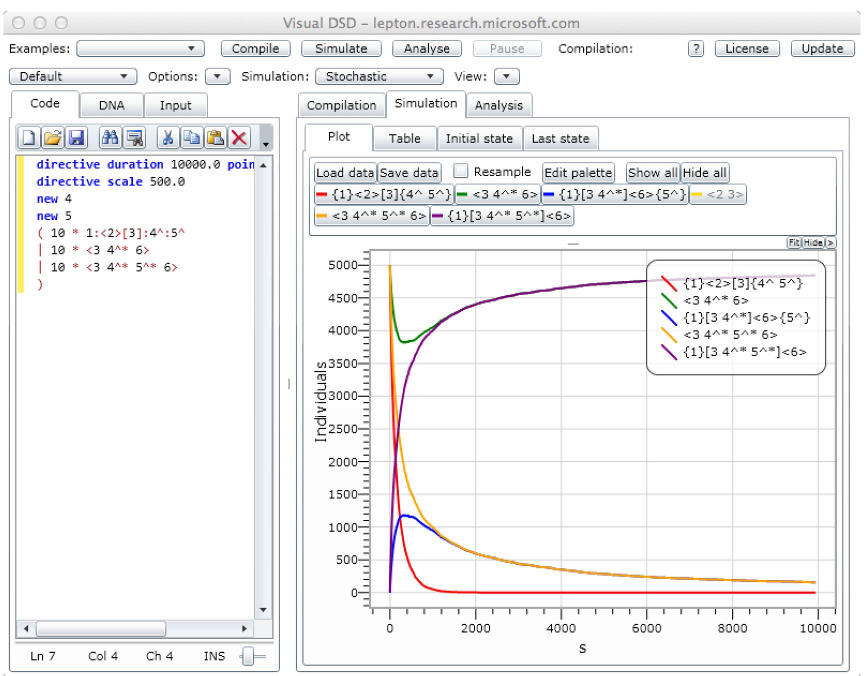

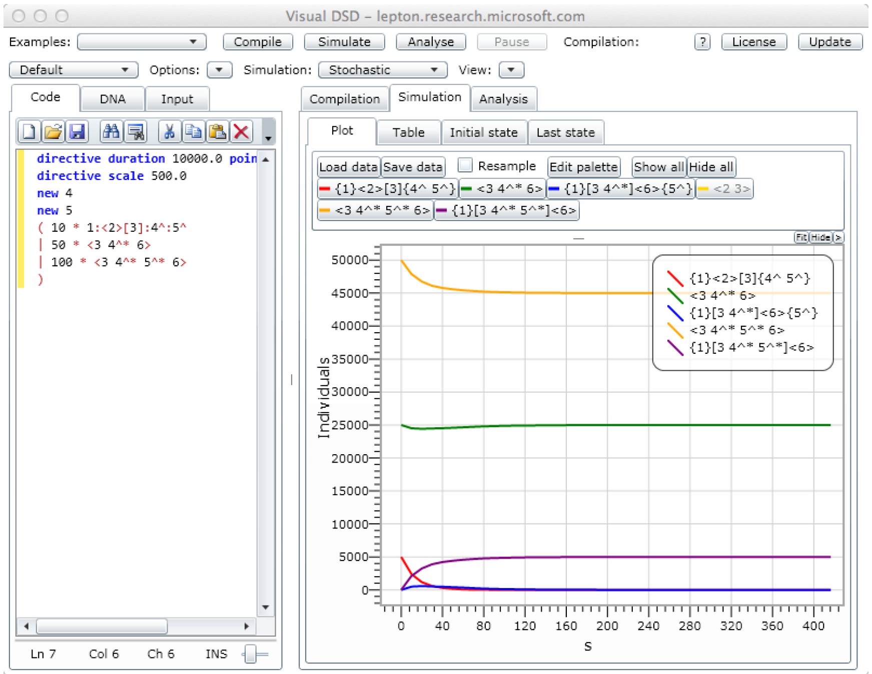

Supplementary Fig. 14: Verification of EPN system in equimolar (top) vs. actual (bottom) stoichiometry.

Supplementary Note 3: Ex-vivo prototyping of robots

Hemocyte extraction:
Insects were anesthetized one by one, by incubation at -20 °C for 7-10 min (depending on animal weight and resilience) in a fresh glass beaker (such that possible secretions from previously frozen insects will not induce stress or unwanted responses). Once an insect has been anesthetized, hemolymph was extracted by puncturing the arthrodial membrane at the base of either metathoracic leg with an ice-cold needle dipped in anti-coagulation buffer (30mM citric acid, 30mM sodium citrate, 1 mM EDTA and 0.05% sodium azide). 25 µL of hemolymph were immediately added to 100 µL of ice-cold anti-coagulation buffer. Prior to ex-vivo experiments, cells were washed once in ice-cold TAE and kept on ice in TAE supplemented with 4 mM Mg^{2+}. Following extraction, hemocytes were counted by flow cytometry and then reconstituted and divided into samples containing approximately 10^4 cells in 50 μL sample. The samples were kept in round bottom 96-well plates on ice until experiment initiation.

Ex-vivo prototyping:
Robots (0.1 pmol of E, plus P1, P2, N, F, and/or P3 in quantities according to the tested stoichiometry) were added to the freshly isolated hemocytes and given 2 minutes at room temperature to equilibrate. Then, protein cues were added in varying concentrations (typically from 1 pM to 10 nM) and the samples were incubated for 2 hours at room temperature. Following incubation, samples were directly analyzed using flow cytometry.

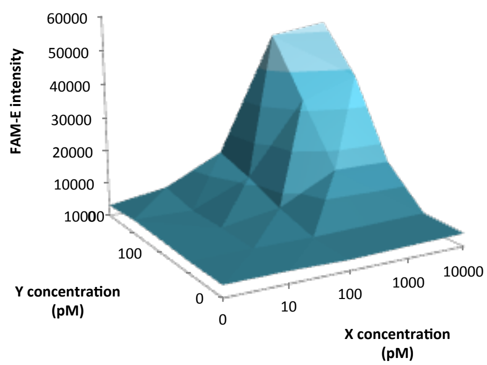

Supplementary Fig. 15: Ex-vivo prototyping of the E (AND) architecture. FAM-tagged E robots mixed with freshly isolated hemocytes were incubated in the presence of both protein cues (X, PDGF; Y, VEGF) in 25 combinations representing all the possible concentrations of X and Y from 0 to 10 nM. Each sample was analyzed by flow cytometry. Each point in the graph represents a sample. Height on the Y axis represents median fluorescence intensity measured by flow cytometry.

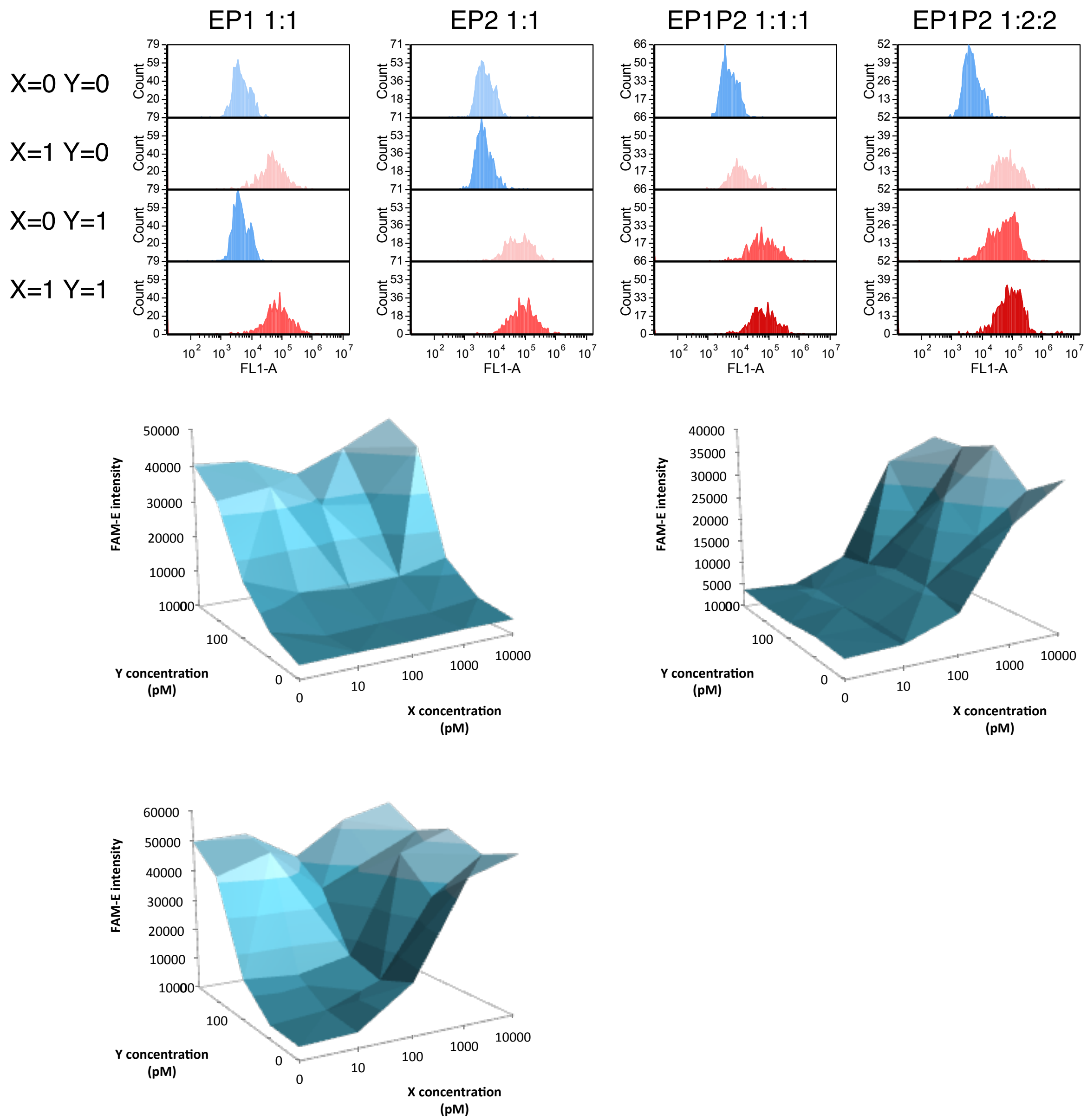

Supplementary Fig. 16: Ex-vivo prototyping of EP1, EP2, and EP1P2 (OR) architectures. EP1 and EP2 were prototyped separately prior to EP1P2, to verify that the addition of either one renders E robots responsive to one cue alone (X or Y). After determining the efficient E:P ratios (found to be 1:>2:>2, shown in the top panel), combinatorial incubation of the EP1P2 architecture with X and Y followed and analyzed by flow cytometry.

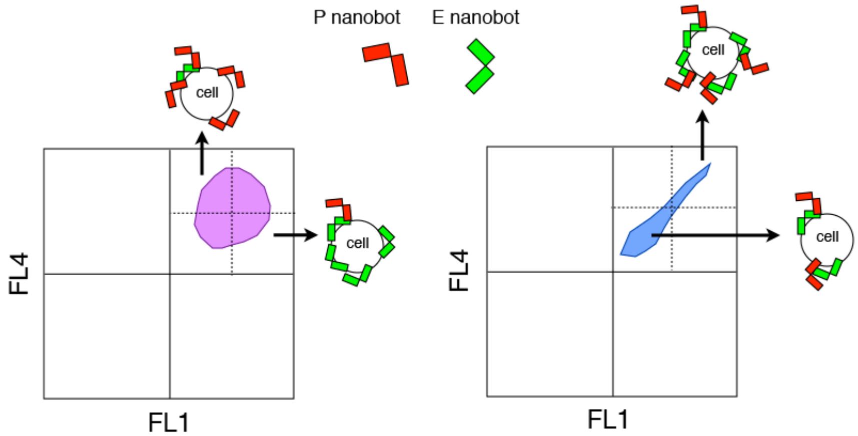

Supplementary Fig. 17: Slanting pattern indicating EP complexes. This scheme explains how can the existence of EP complexes be concluded from slanted populations in flow cytometry. Cells, either primary or lines, that are double-stained in flow cytometry (e.g. for the expression of two surface markers) tend to present as spherical populations (left panel). The spherical pattern indicates that the population is heterogenous, consisting of cells expressing high levels of marker A with low levels of marker B as well as cells expressing high levels of marker B with low levels of marker A. In our system this cannot occur because robot interactions (e.g. between E and P) are approximately always 1:1, so any real pattern generated by robots will consist solely of equal quantities of both species, as shown on the right. Slanting in double-stained cells usually derive from signal leakage due to insufficient compensation. However, in our observations the slanting is preserved even at high compensation levels, indicating that they are robot-derived.

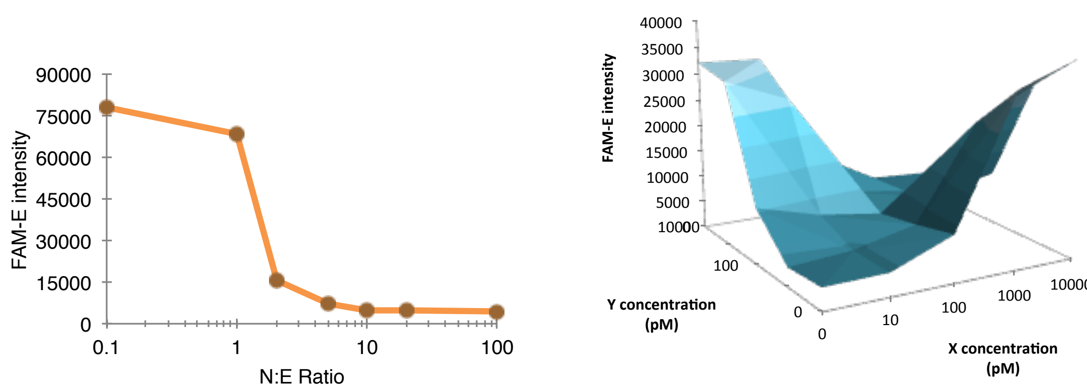

Supplementary Fig. 18: Ex-vivo prototyping of the EP1P2N (XOR) architecture. We first sought to define the N:E stoichiometry in which N efficiently inactivates E. For this, E robots were mixed with varying quantities of N robots making up ratios ranging from 0.1 to 100 (the baseline activity of E was statistically identical to that of E at a 0.1 stoichiometry) in the presence of 10 nM of both protein cues. Complete inactivation of E by N robots was observed at a molar excess of 10 N over E. Using this ratio, EP1P2N architecture was effectively emulated a XOR gate (right panel).

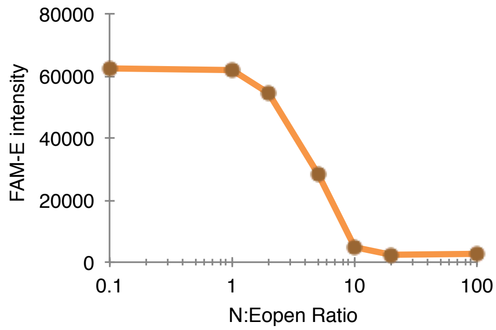

Supplementary Fig. 19: Ex-vivo prototyping of the E_{open}N (NAND) architecture. To examine whether this stoichiometry is different than the one measured and shown in **Supplementary Fig. 18**, we repeated this experiment but with E_{open} in the absence of protein cues (E_{open} contains only complementary gate strands but no sensing strands and are therefore constitutively open). Here, too, the efficient N:E ratio was observed to be 10, and this ratio was chosen in testing the architecture.

Supplementary Note 4: Animal model techniques and analysis:

A highly desired goal is to perform computing in a living animal. The insect *Blaberus discoidalis* was chosen as model animal for various reasons, including simplicity, previous experience with closely related models, and availability of reliable custom made reagents[4]. The hemolymph of *B. discoidalis* expresses negligible nuclease activity and contains large amounts of free DNA as reported for other Dictyoptera[5], and its salt/metal composition is compatible with DNA origami structures (Weidler & Sieck, 1977). We prototyped the robots first ex-vivo on freshly extracted insect hemocytes, with fluorescently-tagged robots loaded with anti-insect hemocyte antibodies as the effector payload.

Animal maintenance:

Adult *Blaberus discoidalis* of both sexes (purchased from Meital Laboratories, Israel) were housed at room temperature and humidity in large plastic containers, and fed with dry dog food, fresh fruit and water *ad libitum*. Egg cartons were used as light shelters. Maximum number of insects per cage was 12.

Injection protocol:

Insects were anesthetized one by one, by incubation at -20 ^{o}C for 7-10 min (depending on animal weight and resilience) in a fresh glass beaker (such that possible secretions from previously frozen insects will not induce stress or unwanted responses). Once an insect has been anesthetized, a 10 μL solution of robots (0.1-3 pmol depending on architecture) in TE containing 4 mM Mg^{2+}, was injected into the hemocoel using a Hamilton syringe. Injection was carried out through the soft membrane between the two last abdominal sternites close to the lateral body margin. Following injection, insects were left to recuperate for up to 4 hours.

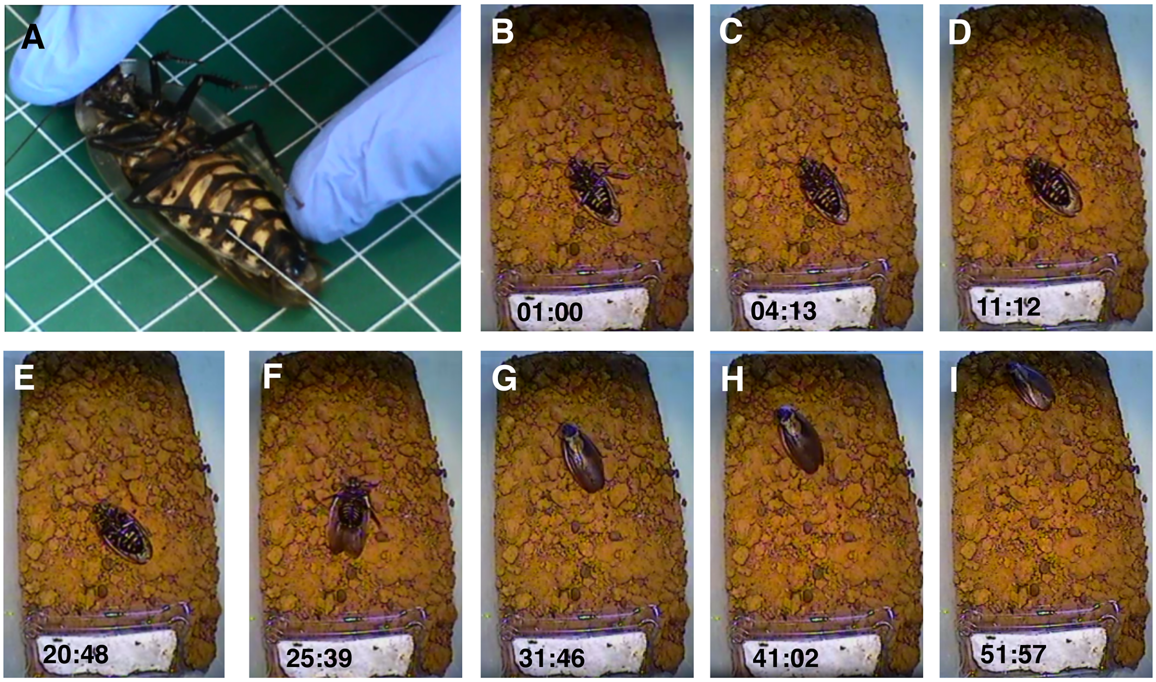

Supplementary Fig. 20: Video caps before and after injection to the insect.

Hemolymph exatraction:

Hemolymph samples were extracted as described in Supplementary Note 3.

Isolation of hemolymph DNA:

Hemolymph DNA isolation was carried out using Qiagen's DNeasy Blood & Tissue Kit according to the manufacturer's instructions **(Supplementary Fig. 21).**

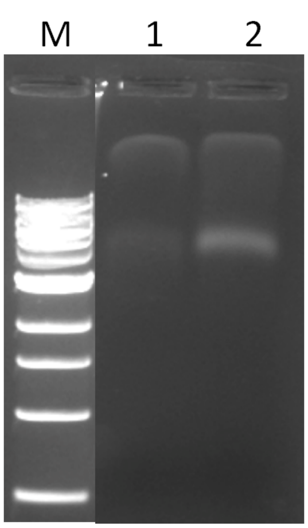

Supplementary Fig. 21: DNA in cockroach hemolymph. Sample migration pattern on a 1% agarose gel. Shown are samples from two different insects.

Nuclease activity assay:

Flow cytometric analysis was carried out to measure nuclease activity in the hemolymph over time. DNA oligos have the following sequences:

/5BioTEG/TTTACTCAGGGCCCTGCAATTGATACTCGAGCAATGGACAGTTA
/5Cy5/TTTAACTAGTCCATTGCTCGAGATATCAATTGCAGGGCCCTGAGTA

were purchased from Integrated DNA Technologies. Sequences were designed to complement each other, generating a potential recognition site for over 40 potential site-specific nucleases as well as DNase I (**Supplementary Fig. 22, panel a**). The duplex is adsorbed onto streptavidin-coated polystyrene microparticles according to the manufacturer's instructions.

Flow cytometry:
Flow cytometry was performed on a dual-laser Accuri A6 flow cytometer and analyzed by FCS Express 4.0 software.

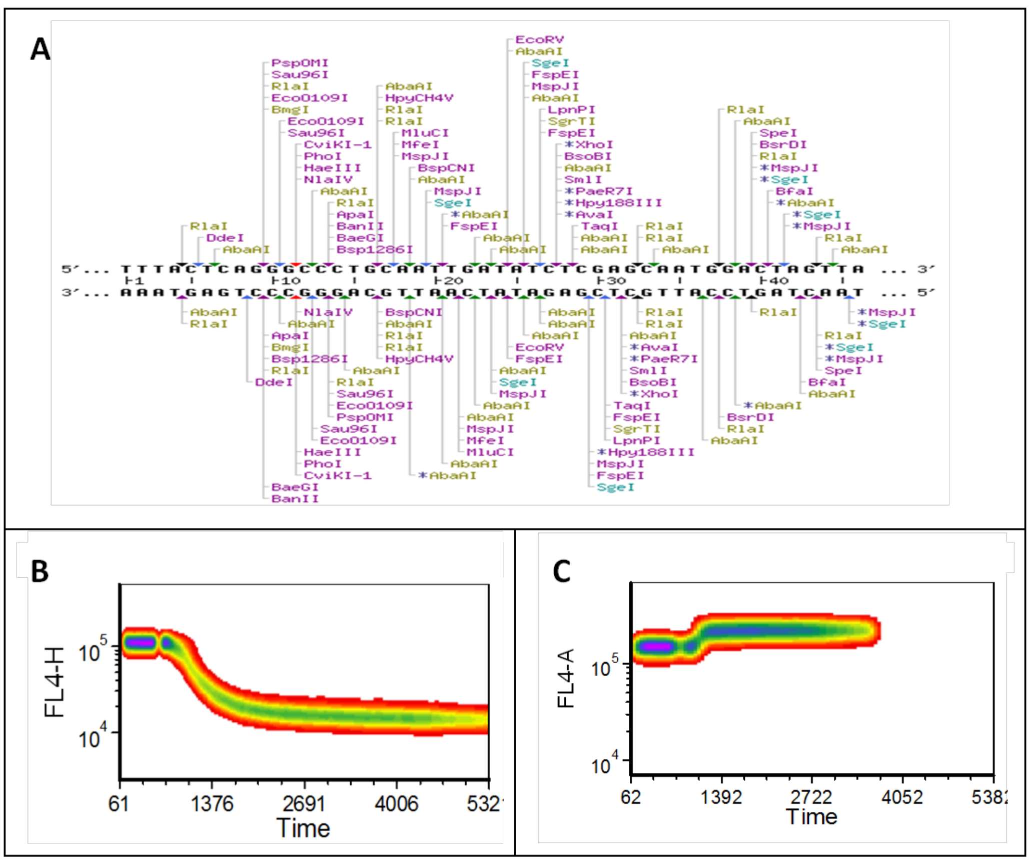

Supplementary Fig. 22: Nuclease activity in hemolymph. A) Restriction map, generated with NEBcutter V2.0 (http://tools.neb.com/NEBcutter2), of dsDNA sequence used in assay, showing over 40 different potential nucleases restriction sequences. **B)** Positive control of beads-bound sequences incubated with XhoI at time t=1 min, as measured by flow cytometry. **C)** beads-bound sequences incubated with freshly-extracted, undiluted hemolymph at t=1 min, as measured by flow cytometry. Time scale is in 0.1 sec. The slight increase in fluorescence in **C** represents aggregation of polystyrene microparticles mediated by hemolymph proteins, which are not present in **B**, however regardless to this aggregation, nuclease activity should have resulted in decreased fluorescence per event over time as seen in **B**.

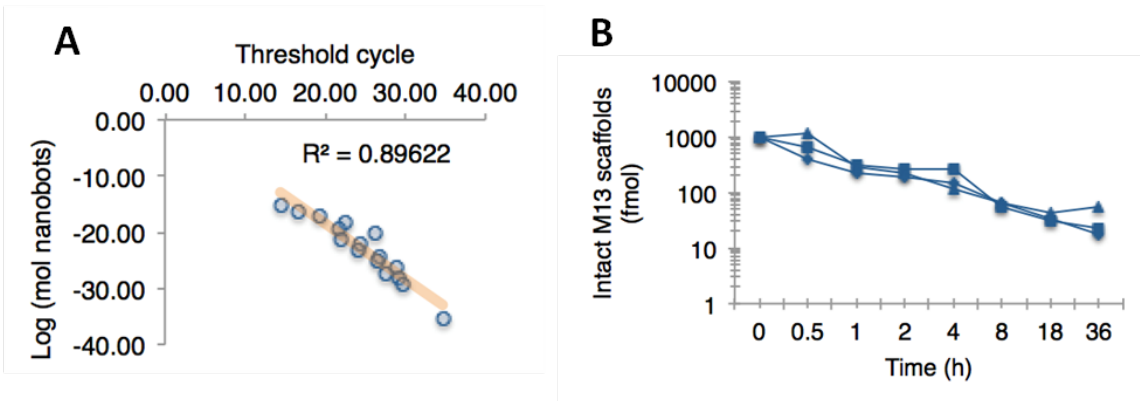

Supplementary Fig. 23: Robot quantification in hemolymph. Robots were quantified in hemolymph using quantitative PCR performed with a TaqMan probe complementary to a region of the M13mp18 scaffold strand that spans one of the chassis axes. A) Calibration curve was generated by performing the qPCR assay on samples containing known quantities of robots (serially diluted, left). B) 1 pmol robots were mixed into undiluted freshly-extracted hemolymph, and at the designated time points DNA was isolated by centrifugal filtration on Amicon 100K (15,000 g, 15 min) and qPCR was performed. Results from hemolymph extracted from 3 different insects are shown (square, triangle and rhombus).

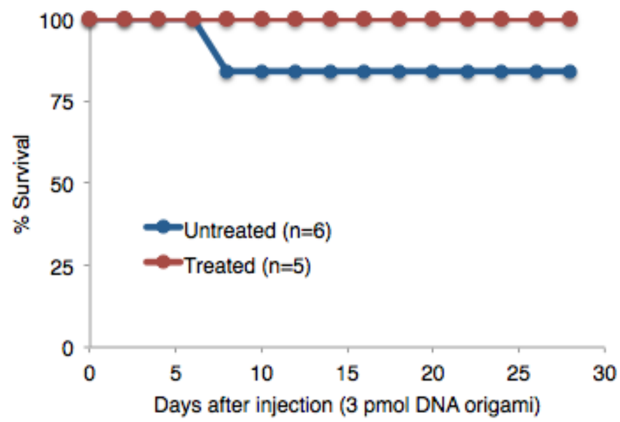

Supplementary Fig. 24: Cockroach survival following robot injection. Cockroaches were injected with 3 pmol robots as described above, housed in separate cages and counted every 2 days, with another untreated group as a control. One animal in the untreated group died of natural causes during the experiment, which was the only death documented in the two groups.

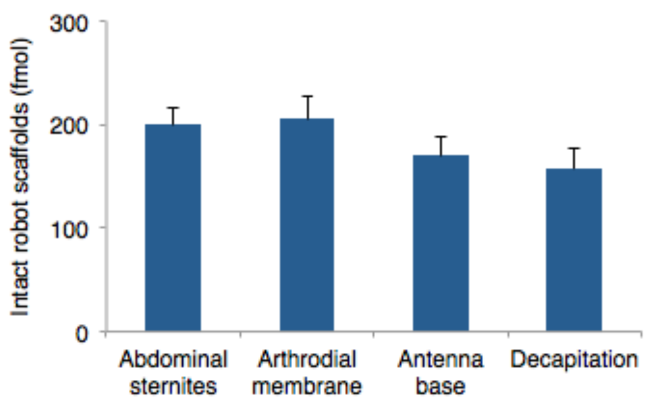

Supplementary Fig. 26: Distribution of robots in the cockroach following injection. Robots (1 pmol) were injected to cockroaches (n=3). Animals were sacrificed at t=1 h and scaffold strands were counted by qPCR in samples drawn from various locations in the cockroach body – between the abdominal sternites (location of injection), the left arthrodial membrane, base of left antenna, and following decapitation of the animal.

Supplementary Note 5: Statistical mechanics of robots in insect hemocoel

Fluorescence Correlation Spectroscopy[6-7]:

Fluorescence Correlation Spectroscopy (FCS) measurements were performed on a MicroTime 200 single molecule fluorescence lifetime measurement system (PicoQuant, GmbH Berlin, Germany) and the setup consists of an inverse Olympus IX 71 microscope. As excitation source, a ps pulsed–diode laser, set at repetition rate of 40 MHz and emitting at wavelength 635 nm (LDH-P-C-640B, PicoQuant GmbH Berlin Germany), was used, which fits well to the excitation of the Cy5 dye.
The presented measurements were performed at a depth of approx. 100 μm inside a drop of solution (on top of a cover-slip glass) which contains the sample, a 15 μL vol. at concentrations of the fluorescent sample in the 0.1-1.0 nM range. Fluorescence from the excited molecules was collected with the same objective, and focused with an achromatic lens (f = 175 mm) onto a 50 μm diameter pinhole. The fluorescence emissions was selected by a 690/70 nm Band-pass filter (HQ690/70, Chroma Technology Corp. Rockingham Vermont, USA). The detector was a single photon avalanche photodiodes (SPAD) (170 μm, Perkin Elmer SPCM-AQRH 13).
The data were correlated by the HydraHarp400 Time Correlated Single Photon Counting (TCSPC) system and collected with SymphoTime version 5 (both by PicoQuant GmbH Berlin, Germany).

The fluorescence autocorrelation function (ACF), $G(\tau)$, is defined as

$$G(\tau) = \frac{\langle \delta F(t) \cdot \delta F(t+\tau) \rangle}{\langle \delta F(t) \rangle^2} \quad \delta F(t) = F(t) - \langle F(t) \rangle \quad (1)$$

where $F(t)$ is the fluorescence at time t, brackets denote time averages, and τ is the time between each pair of detected photons. The contribution of detector afterpulsing was removed using the Fluorescence Lifetime Correlation Spectroscopy (FLCS) harnessing the extra information from Cy5 fluorescence decays. The data were fit using a triplet corrected autocorrelation function, $G(\tau)$, as shown in the analytical form in Eq. 2:

$$G(\tau) = \frac{1}{\langle N \rangle}\left(1 - T + Te^{-\frac{\tau}{\tau_T}}\right)\frac{1}{\left(1 + \frac{\tau}{\tau_D}\right)\left(1 + \frac{\tau}{\kappa^2 \tau_D}\right)^{1/2}} \quad (2)$$

T is the amplitude of the triplet blinking process, τ_T is the apparent triplet blinking relaxation time of the dye, τ_D is the mean 3D free diffusion time of the molecule (nanorobot) in the focal volume, and <N> is the mean number of emitting molecules in the focal volume. The factor, κ, describes the 3D Gaussian focal volume in terms of the axial to radial ratio and is calculated from measurements of the standard dye Atto 647N with a known diffusion coefficient of 400 $\mu m^2/s$ at 298 ^{0}K.

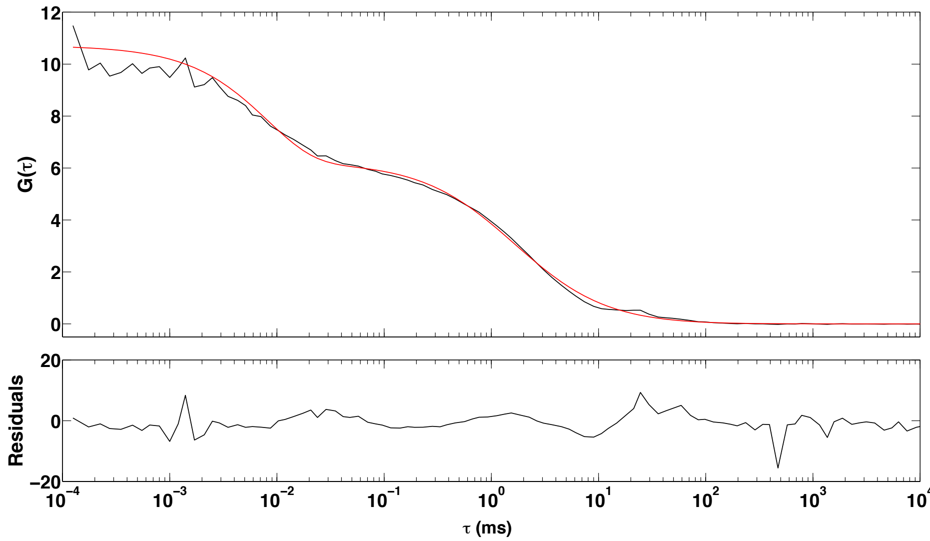

Supplementary Fig. 26: Correlation function data. Typical data obtained in the FCS experiments with closed nanorobots in 40 mM Tris-Acetate buffer, 8 mM $MgCl_2$, pH 8. The experimental data (black curve) were fit to triplet corrected autocorrelation function model (red curve) as described in the text, and the residual distribution for the fit is shown in the bottom panel.

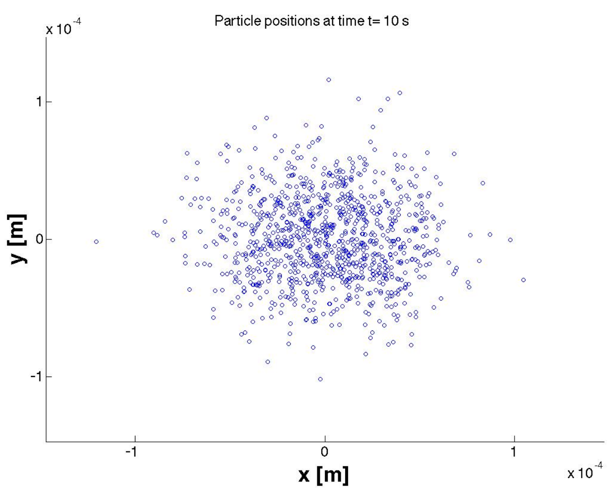

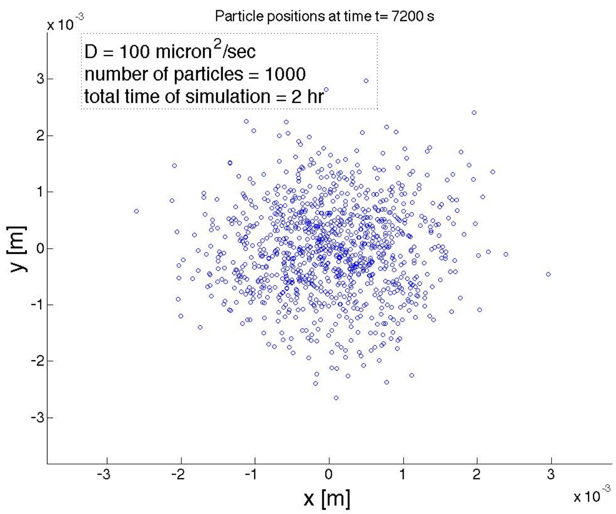

Supplementary Fig. 27: Simulated diffusion of robots without mixing. In this simulation virtual, very small robots with diffusion coefficient of 100 microns^2/sec were injected into a central spot and allowed to diffuse for 10 seconds and 2 hours. Even after 2 hours of diffusion without mixing, robots are not expected to diffuse more than 3 mm to each direction. Therefore mixing is necessary, as in the case of the open circulatory system of *B. discoidalis*.

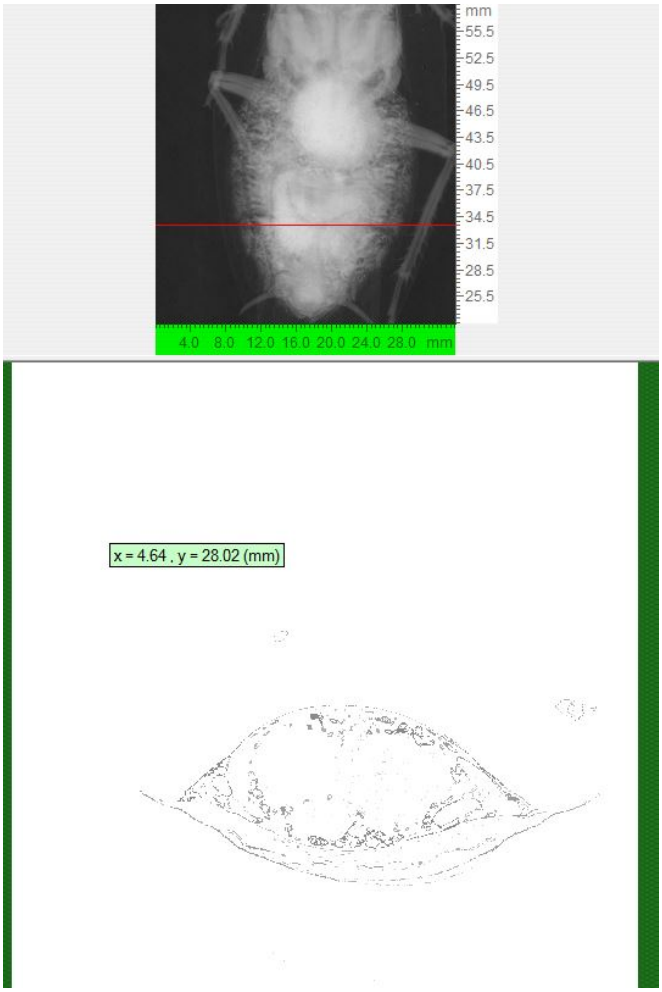
mm
55.5
52.5
49.5
46.5
43.5
40.5
37.5
34.5
31.5
28.5
25.5
4.0 8.0 12.0 16.0 20.0 24.0 28.0 mm
x = 4.64 , y = 28.02 (mm)

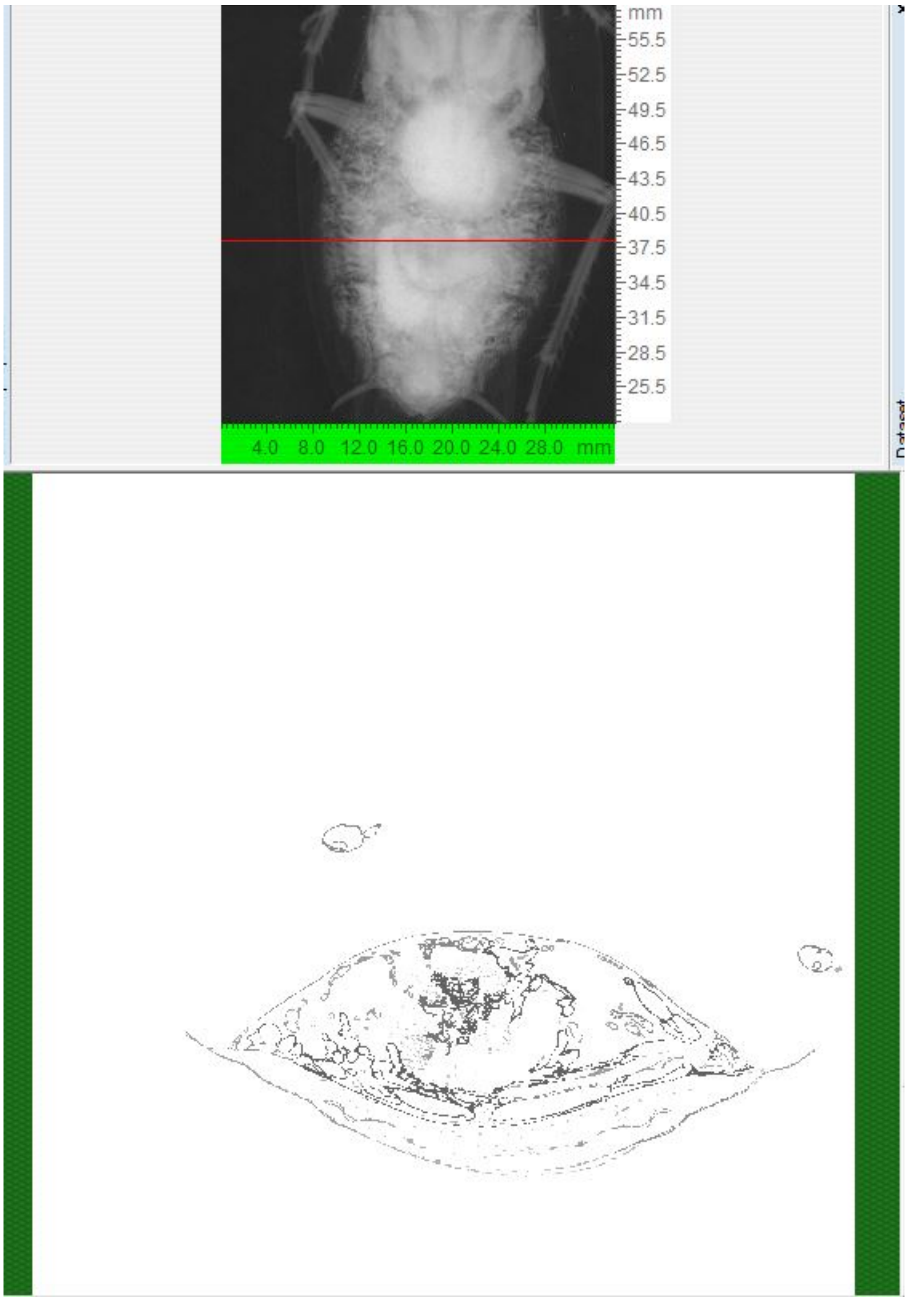
mm
55.5
52.5
49.5
46.5
43.5
40.5
37.5
34.5
31.5
28.5
25.5
4.0 8.0 12.0 16.0 20.0 24.0 28.0 mm

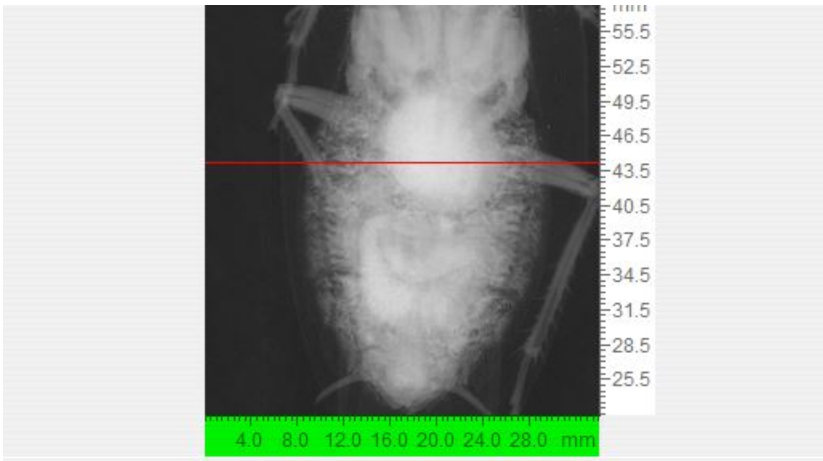
55.5
52.5
49.5
46.5
43.5
40.5
37.5
34.5
31.5
28.5
25.5
4.0 8.0 12.0 16.0 20.0 24.0 28.0 mm

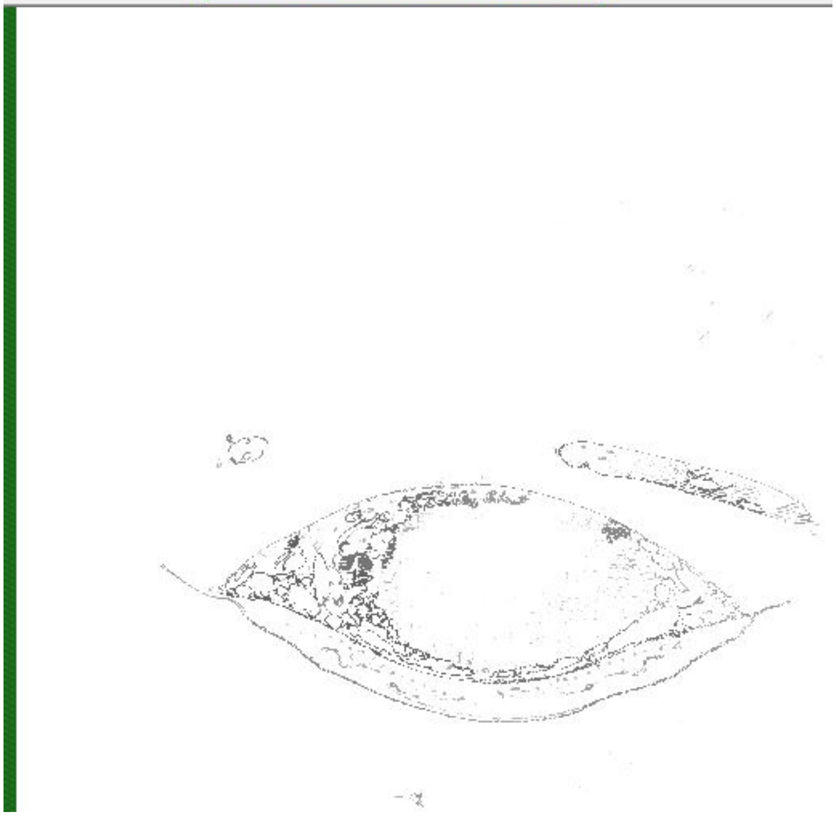

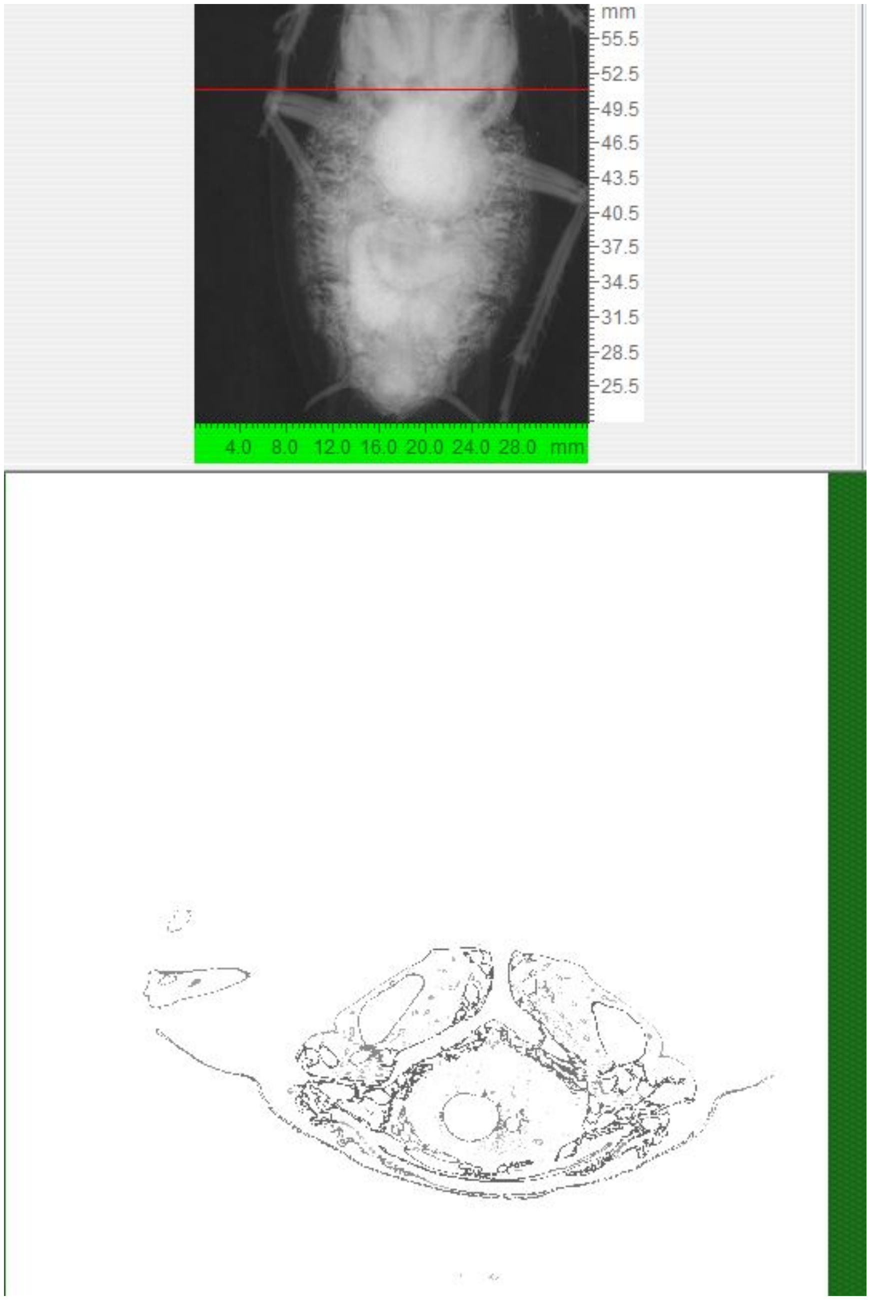

Figure S28: Calculation of the hemolymph space from CT scans.

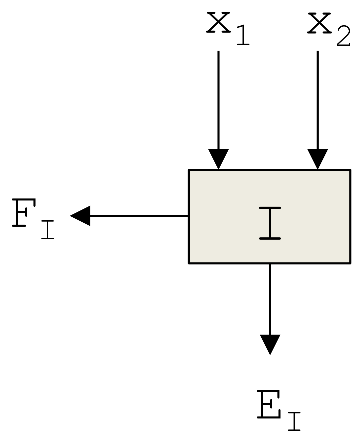

x_1	x_2	E_I	F_I
0	0	0	0
1	0	1	0
0	1	1	0
1	1	0	1

Figure S29: Scaling-up half-adders to create n-bit ripple carry adders. The basic half-adder architecture consists of 5 robots (E, F, P1, P2, N), receiving two input molecules (x1 and x2) and produces two outputs (robot states), which can be either closed (0) or open (1). A closed state is a dead-end and does not key further robots, while the open state has two functions: it exposes a therapeutic molecule, and relays a key sequence to the next robot. Each therapeutic molecule is tagged with a different color, so the number of distinct color combinations represents the number of therapeutic molecules or combinations of them which are producible by this group of robots.

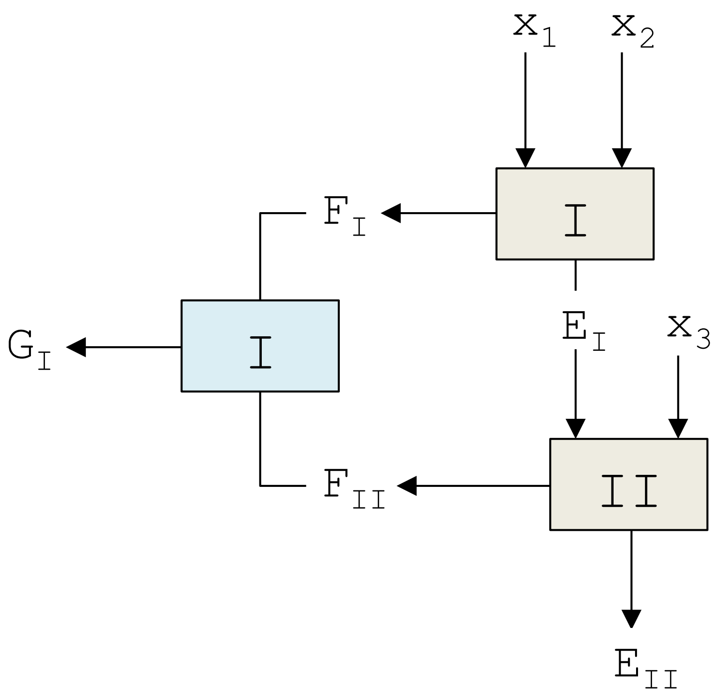

x_1	x_2	E_I	F_I	x_3	E_{II}	F_{II}	G_I
0	0	0	0	0	0	0	0
0	0	0	0	1	1	0	0
1	0	1	0	0	1	0	0
1	0	1	0	1	0	1	1
0	1	1	0	0	1	0	0
0	1	1	0	1	0	1	1
1	1	0	1	0	0	0	1
1	1	0	1	1	1	0	1

Fig. S29 (continued): Combining two half adder generates a full adder which receives 3 inputs (two molecules and a key from the original half-adder) and produces 2 output robots. These can again activate a therapeutic molecule simultaneously with keying the next robot. The “carry bit” robot F(I) (from the original half adder) and the “carry bit” robot F(II) from the second half adder are fed into an OR gate consisting of 3 robot types (G, P3, P4). The resulting G robot, with the “sum bit” robot from the second half adder E(II), now form the two outputs of the full adder.
In terms of robot complexity, adding the second half adder required 8 additional robots - 5 in the half adder, 3 in the OR gate.

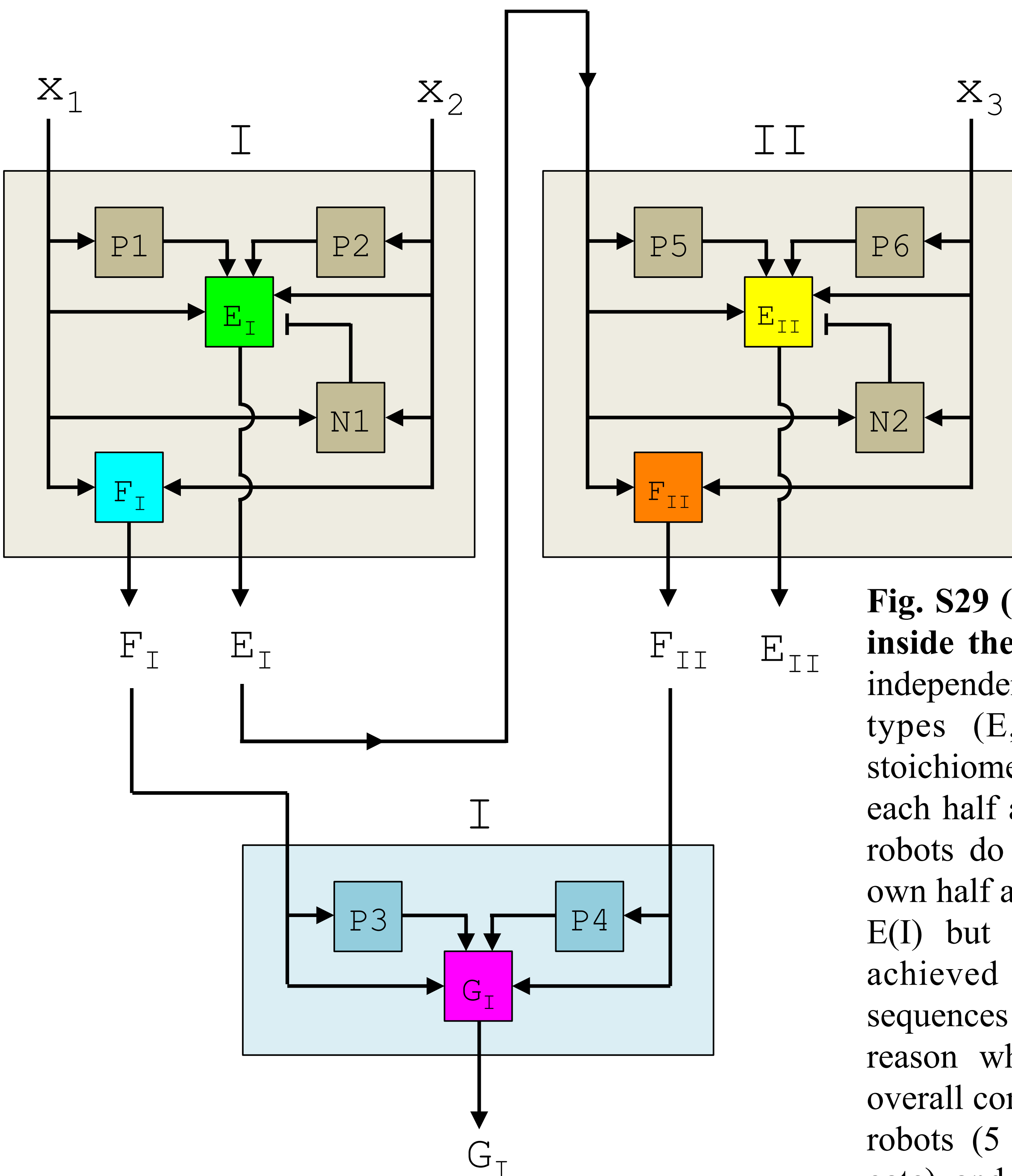

Fig. S29 (continued): Robot wiring scheme inside the full adder. Each half adder is an independent system consisting of 5 robot types (E, F, P1, P2, N) at a certain stoichiometry (1:1:5:5:10 respectively). In each half adder, N can negate E but not F. N robots do not negate robots outside of their own half adder, so for example N1 can negate E(I) but not E(II). In-adder specificity is achieved by designing specific toehold sequences for key-gate pairs. This is the reason why each half adder increases the overall complexity of the system linearly by 8 robots (5 for the half adder, 3 for the OR gate), and not exponentially.

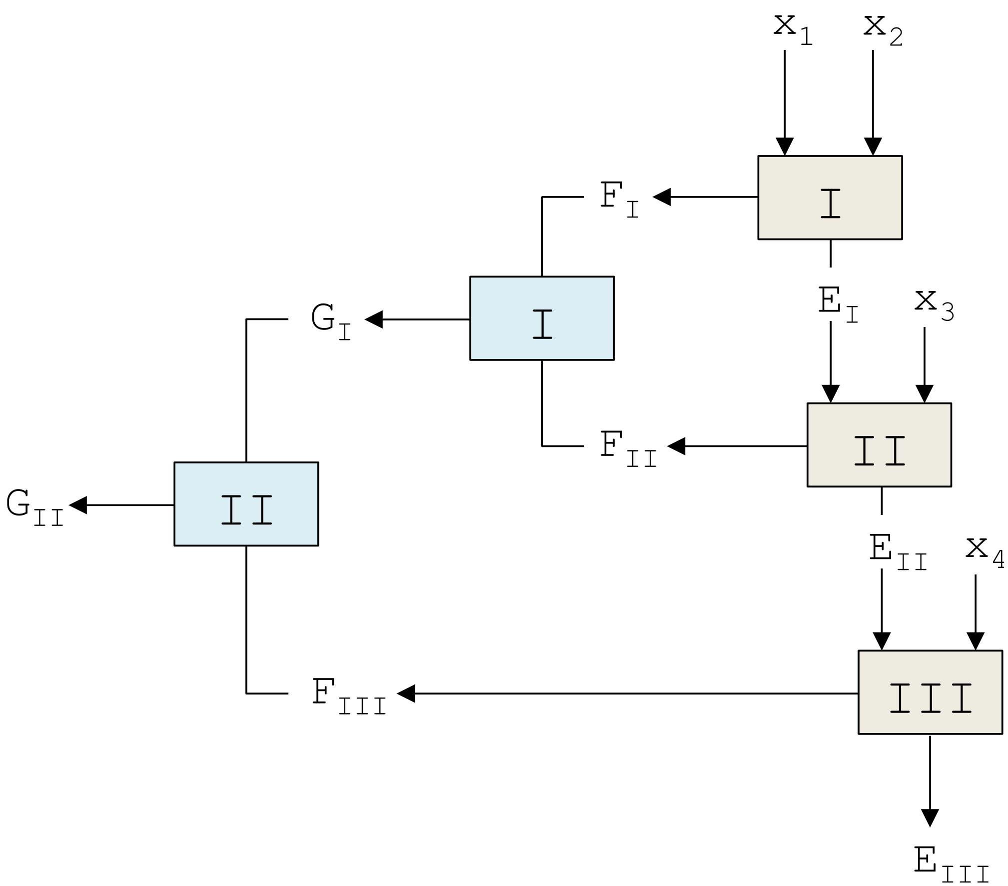

x_1	x_2	E_I	F_I	x_3	E_{II}	F_{II}	G_I	x_4	E_{III}	F_{III}	G_{II}
0	0	0	0	0	0	0	0	0	0	0	0
0	0	0	0	1	1	0	0	0	1	0	0
1	0	1	0	0	1	0	0	0	1	0	0
1	0	1	0	1	0	1	1	0	0	0	1
0	1	1	0	0	1	0	0	0	1	0	0
0	1	1	0	1	0	1	1	0	0	0	1
1	1	0	1	0	0	0	1	0	0	0	1
1	1	0	1	1	1	0	1	0	1	0	1
0	0	0	0	0	0	0	0	1	1	0	0
0	0	0	0	1	1	0	0	1	0	1	1
1	0	1	0	0	1	0	0	1	0	1	1
1	0	1	0	1	0	1	1	1	1	0	1
0	1	1	0	0	1	0	0	1	0	1	1
0	1	1	0	1	0	1	1	1	1	0	1
1	1	0	1	0	0	0	1	1	1	0	1
1	1	0	1	1	1	0	1	1	0	1	1

Fig. S29 (continued): Adding a third half adder requires, again, the addition of 8 robots - 5 in the third half adder, 3 in the second OR gate. It is evident therefore that each half adder requires 8 new robot types, and increases the capacity of the system to control therapeutic molecules by 3 additional molecules.

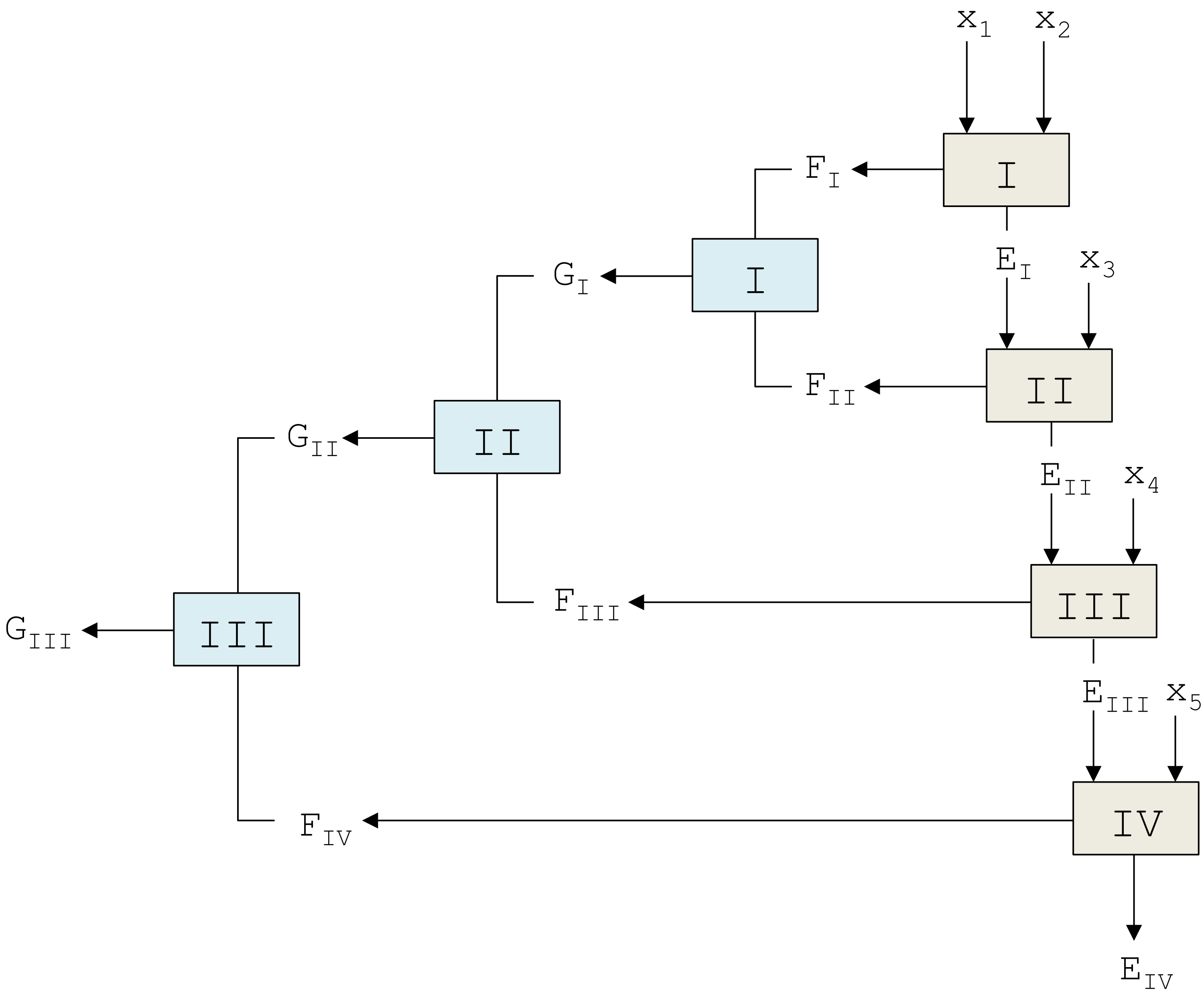

Fig. S29 (continued): An example of a 2-bit ripple carry adder, requiring 29 different types of robots and capable of generating combinations of 11 therapeutic molecules in response to 5 biomarkers.

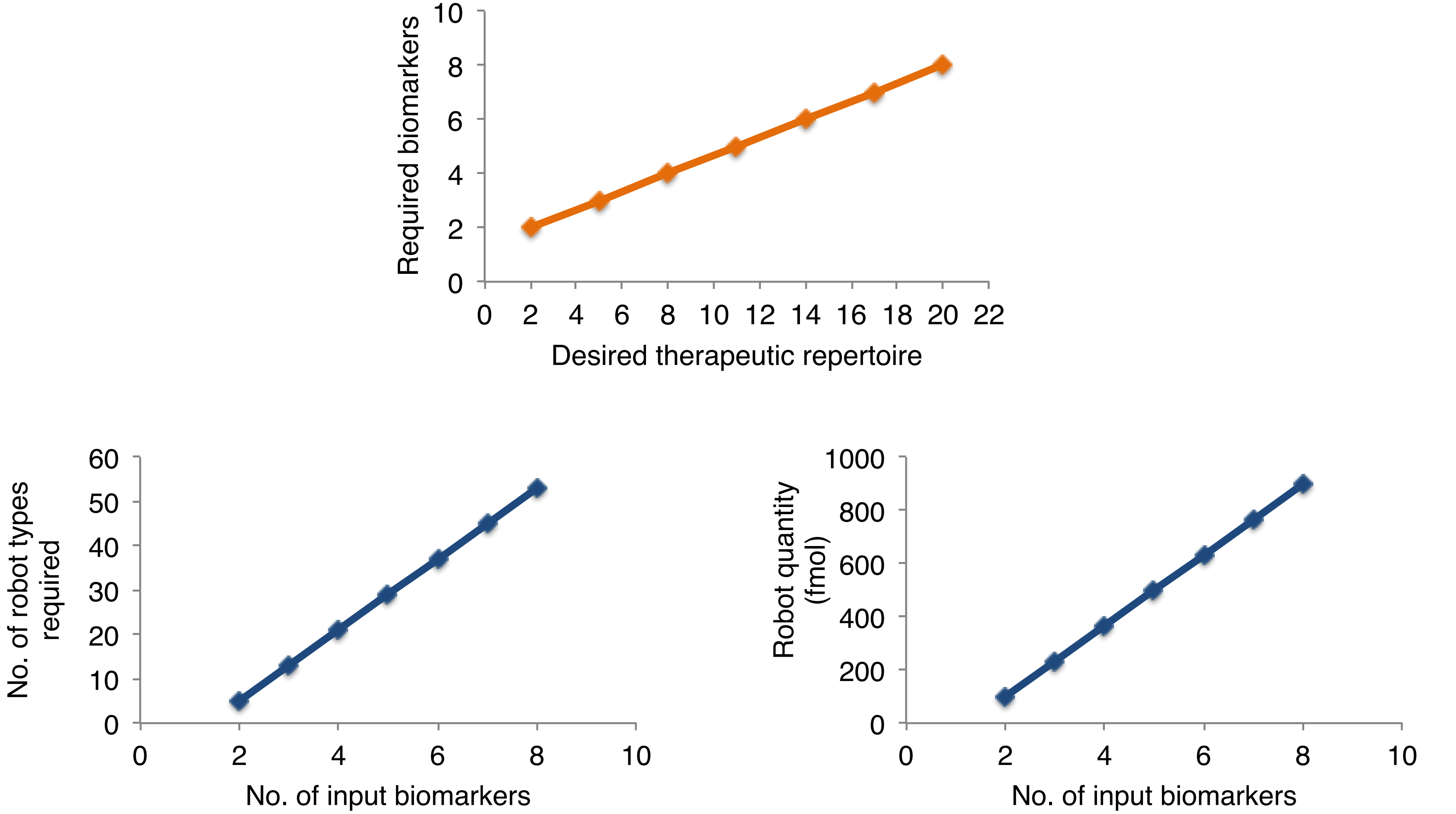

Fig. S30: Scaling, complexity, and capacity in the half adder based system presented here. The complexity rises as the number of therapeutic molecules in the chosen repertoire increases. However the scaling is linear and not exponential. Bottom graphs show the different robot types required and their quantity in fmol (fit for insect system presented here) as a function of chosen repertoire size.

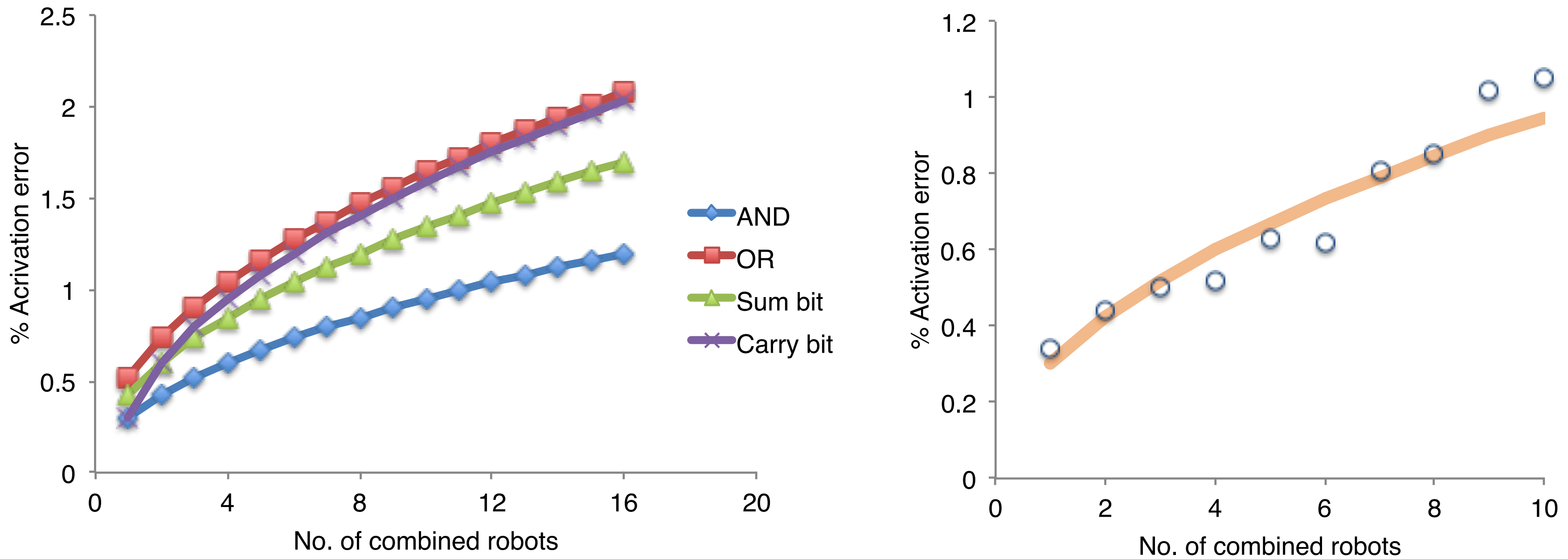

Fig. S31: Expected vs. measured error propagation in a scaled robot system. Robot activation errors (measured as % of targets engaged by robots in the complete absence of input) scaled at an order of the root sum square of the combined errors from all robots linked within the logical operator. Left: theoretical error propagation based on RSS of combined robot errors. Right: measured errors from 10 AND robots combined such that each keys the next; blue circles represent measurements, orange trend line represent expected propagation of combined AND robots.

References

1. Green, LS et al. Inhibitory DNA ligands to platelet-derived growth factor B-chain. *Biochemistry* **35**, 14413-14424 (1996).
2. Kaur, H, Yung, LY. Probing high affinity sequences of DNA aptamer against VEGF165. *PLoS One* **7**, e31196 (2012).
3. Castro, CE et al. A primer to scaffolded DNA origami. *Nat. Methods* **8**, 221-229 (2011).
4. Bulmer, MS, Bachelet, I, Raman, R, Rosengaus, RB, Sasisekharan, R. Targeting an antimicrobial effector function in insect immunity as a pest control strategy. *Proc. Natl. Acad. Sci. USA* **106**, 12652-12657 (2009).
5. Garbutt, JS, Belles, X, Richards, EH, Reynolds, SE. Persistence of double-stranded RNA in insect hemolymph as a potential determiner of RNA interference success: Evidence from Manduca sexta and Blattella germanica. *J. Insect Physiol.* **59**, 171-178 (2013).
6. Magde, D, Elson, E, Webb, WW. Thermodynamic fluctuations in a reacting system: measurement by fluorescence correlation spectroscopy. *Phys. Rev. Lett.* **29**, 705–708 (1972).
7. Korlann Y, Dertinger T, Michalet X, Weiss S, Enderlein J. Measuring diffusion with polarization-modulation dual-focus fluorescence correlation spectroscopy. *Opt. Express.* **16**, 14609–14616 (2008).